AD NUMBER

AD867575

LIMITATION CHANGES

TO:

Approved for public release; distribution is unlimited.

FROM:

**Distribution authorized to U.S. Gov't. agencies and their contractors;
Administrative/Operational Use; DEC 1969. Other requests shall be referred to Army Aviation Materiel Labs., Fort Eustis, VA.**

AUTHORITY

USAAMRL ltr 23 Jun 1971

AD

USAAVLABS TECHNICAL REPORT 69-70

EXPERIMENTAL INVESTIGATION OF SUPERCONDUCTING SYNCHRONOUS MACHINES

By

J. C. LaFrance

E. J. Lucas

J. Teno

December 1969

U. S. ARMY AVIATION MATERIEL LABORATORIES
FORT EUSTIS, VIRGINIA

CONTRACT DA 44-177-AMC-410(T)
AVCO EVERETT RESEARCH LABORATORY
A DIVISION OF AVCO CORPORATION
EVERETT, MASSACHUSETTS

79

Disclaimers

The findings in this report are not to be construed as an official Department of the Army position unless so designated by other authorized documents.

When Government drawings, specifications, or other data are used for any purpose other than in connection with a definitely related Government procurement operation, the United States Government thereby incurs no responsibility nor any obligation whatsoever; and the fact that the Government may have formulated, furnished, or in any way supplied the said drawings, specifications, or other data is not to be regarded by implication or otherwise as in any manner licensing the holder or any other person or corporation, or conveying any rights or permission, to manufacture, use, or sell any patented invention that may in any way be related thereto.

Disposition Instructions

Destroy this report when no longer needed. Do not return it to the originator.

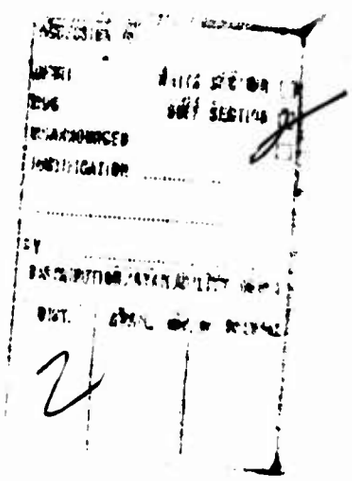

DEPARTMENT OF THE ARMY
HEADQUARTERS US ARMY AVIATION MATERIEL LABORATORIES
FORT EUSTIS, VIRGINIA 23604

The work done under this contract is a portion of the overall project to investigate new ideas and concepts which might offer advantages in future propulsion systems for Army aircraft.

Work sponsored by the Air Force and prior Army contracts established the feasibility of superconducting generators. This study indicates that superconducting motors also are technically feasible.

Task 1G162204A01410
Contract DA 44-177-AMC-410 (T)
USAAVLABS Technical Report 69-70
December 1969

EXPERIMENTAL INVESTIGATION OF SUPERCONDUCTING SYNCHRONOUS MACHINES

Final Report

By

J. C. La France
E. J. Lucas
J. Teno

Prepared by

Avco Everett Research Laboratory
a Division of
Avco Corporation
Everett, Massachusetts

for

U. S. ARMY AVIATION MATERIEL LABORATORIES
FORT EUSTIS, VIRGINIA

ABSTRACT

This report details the design and testing of a synchronous motor with superconducting field and armature windings. Data are furnished on the performance of the superconducting field and armature windings. The open-circuit characteristics and terminal characteristics of the loaded machine operating as a generator with its armature in LN_2 and in the superconducting state are given. Data are given on the machine operated as a synchronous motor. The measured machine parameters are compared to the predictions of Avco's Final Report on Contract No. Nobs-94528, "Study of Potential Size and Weight Reductions in Marine Electric Propulsion Machine by Utilizing Superconductors". The design for a number of 3000-hp motors with superconducting field winding is given.

TABLE OF CONTENTS

	Page
ABSTRACT	iii
LIST OF ILLUSTRATIONS	vi
LIST OF TABLES	viii
I. INTRODUCTION	1
II. EXPERIMENTAL PROGRAM	3
A. Design of Experimental Superconducting Machine	3
B. Test Rig	23
C. Experimental Results	28
III. MACHINE DESIGN	37
A. Introduction	37
B. Preliminary Machine Designs	37
C. Cryogenic Design	43
D. Mechanical Design	54
E. Conformance to Military Specifications	56
LITERATURE CITED	61
APPENDIX - CALCULATION OF THE NO-LOAD COPPER LOSSES	63
DISTRIBUTION	69

LIST OF ILLUSTRATIONS

Figure		Page
1	Dewar Arrangement Used in Superconducting Motor .	4
2	Rotor Dewar of Superconducting Motor	5
3	Two-Pole Superconducting Field Winding	7
4	Superconducting Field Winding in Its Banding Container With Attached Vapor-Cooled Leads	8
5	Schematic of Armature Winding Form	9
6	Prediction of Armature Output Voltage Versus Frequency	14
7	H-I Characteristic of Wire Used to Wind the Armature.	16
8	Configuration of Synchronous Machine With Magnetic Shield	20
9	Superconductor Losses Versus Peak Applied Field for the Superconducting Armature.	22
10	Copper Losses Versus Peak Applied Field for the Superconducting Armature	24
11	Total Armature Losses Versus Peak Applied Field .	25
12	Schematic of Test Arrangement.	26
13	Power Out of Armature and Drag of Drive System Versus RPM	27
14	Location of Field Probes on Superconducting Field Winding	29
15	Radial Plot of Field Intensity as a Function of Field Excitation	30
16	Open-Circuit Characteristics Versus Field Excitation	32

LIST OF ILLUSTRATIONS (Contd)

Figure		Page
17	Terminal Characteristics for Unity Power Factor Load	35
18	Current Density Versus Magnetic Field for Superconducting Coils Presently in Use. Shown Also Is the Curve Selected for the Machine Designs Presented in This Report.	41
19	Geometry of General Air Core Machine	42
20	Critical Fields for Various Superconductors	46
21	Phase Diagram for Helium	47
22	A Heater Plot Showing Typical Two-Dimensional Behavior at a Magnet Current of 550 Amperes	49
23	Heater Current at Takeoff and Recovery Versus Helium Pressure at a Magnet Current of 620 Amperes	50
24	Rotary Joint in Liquid Cryogen Transfer Line	51
25	Double-Ended Dewar Design for Superconducting Motor	53
26	Refrigerator Weight Versus Refrigerator Capacity at 4.2°K	55
27	Assembly Layout of Typical Motor With Superconducting Field	59
28	Actual and Assumed Superconductor Cross Sections	64

LIST OF TABLES

Table		Page
I	Summary of Design Equations for a Shielded Synchronous Machine	17
II	Nomenclature for Table I	19
III	Geometric Parameters of Synchronous Alternator . .	21
IV	Calculated Parameters of Synchronous Alternators . .	21
V	Predicted Versus Experimental Values	34
VI	Summary of Design Equations for Synchronous Machines With Armature Outside	39
VII	Summary of Machine Parameters	44
VIII	Synchronous Motor Sizes	45

I. INTRODUCTION

The feasibility of using rotating electrical machines having superconducting field and armature windings as power transmission elements in helicopter drives is evaluated. Two separate items are covered. The first is a description of an experimental program, and the second is an outline of a design for a 3000-hp synchronous machine suitable for use in helicopter drives.

It has been demonstrated that the replacement of all conventional DC windings by superconducting windings is feasible.[1,2] Weight and size advantages result from higher magnetic fields with less need, and in some cases, no requirement at all, for ferromagnetic structures. In short, the DC field winding of the DC machine, including the homopolar machine, and the DC field winding of the AC synchronous machine can be advantageously replaced by superconducting windings. A superconducting winding carrying a direct current is capable of supporting current densities far in excess of those that can be realized in the room temperature field windings of conventional machines. As a consequence, the magnetic flux densities that can be produced with superconducting field windings can far exceed the saturation point of ferromagnetic materials. The need for these materials, other than for purposes of field shaping and shielding, is therefore obviated in a machine making use of superconducting windings. Further, since the power density of a machine is proportional to the square of the field intensity, the reason for the reduction in weight and size becomes obvious.

One object of this work has been to evaluate the feasibility of replacing the AC windings of machines with superconducting windings. Although superconducting transformers have been successfully designed, constructed, and tested,[3,4] past work at Avco[5] has indicated that for alternating field and alternating current conditions, the hysteritic losses of superconductors would be prohibitively high. Note that these tests were done under conditions of stationary AC fields.

In rotating machinery, however, the AC fields have rotating components. The phenomenological theories of hysteresis loss in superconductors, such as the Bean theory[9] and its various modifications, do not analyze the case of a rotating, or sweeping, magnet field. Therefore, it has been necessary to gather data by tests on an actual machine.

The experimental part of this work is concerned with the design, construction, and testing of a machine that would demonstrate some of the basic design concepts for machines with superconducting windings. The aim was not to produce a machine of minimum weight and size but a test-bed to study the rotating superconducting field concepts and to evaluate the performance of a superconducting armature.

Among the relevant features incorporated in the test machine were:

1. The rotating member was located inside the stationary one. This reduced the centrifugal stresses, thereby allowing the machine to operate at higher speeds.

2. The field winding was located on the rotating member. This allowed easier shielding and required that the slip rings transmit only the small amount of power needed for field energizing, and made the problem of field shielding in actual machines much simpler.

3. A heavy laminated iron shield was located around the armature. This straightened the field lines and subjected the whole of the armature winding to a perpendicular magnetic field. The near absence of fringing field in the armature region made this armature behave as though it were part of a much longer (and more powerful) machine. The perpendicular field lines also greatly simplified the loss calculations in the armature.

The decision to use or not to use a superconducting armature winding in the design for the proposed 3000-hp motor had to await the experimental results. Once the necessary data had been obtained, a final design study on a 3000-hp motor was made; the results are presented here.

II. EXPERIMENTAL PROGRAM

A. DESIGN OF EXPERIMENTAL SUPERCONDUCTING MACHINE

1. Cryogenic Design

For greater flexibility in testing, the machine was designed to permit the armature to be operated at various temperatures, including 4.2°K, to allow superconducting operation. This flexibility was achieved at some increase in complexity because the armature had to be enclosed in a Dewar. Since the Dewar walls are exposed to a sweeping magnetic field, they were made of a nonmetallic material to avoid excessive eddy current losses. The field winding was located inside the armature and on the rotor center line.

Figure 1 is a schematic of the Dewar arrangement. The machine contains two Dewars. The superconducting field winding is enclosed in a stainless steel Dewar that also forms the rotor of the machine. The armature is inserted in an annular plastic Dewar that fits around the rotor Dewar. Liquid helium is fed to the rotating superconducting field winding by a stationary fill tube inserted through the hollow top shaft of the machine (see Figure 1).

Because of the low latent heat of vaporization of liquid helium, it is imperative to minimize the heat leak to the liquid helium regions of the Dewars. The accepted procedures are to use materials with poor thermal conductivities and long thermal leak paths (long-necked Dewars) and to use the helium boil-off vapors to cool the Dewar walls to absorb most of the conduction heat leak. Liquid nitrogen shields are used around the liquid helium regions, whenever possible.

In this particular application, the length of the rotor is limited by the necessity to keep the rotor's critical frequency higher than 12,000 rpm. It was also impractical to feed both LN_2 and LHe to the rotating Dewar. The critical frequency criterion allowed about 4 inches of neck length on each side of the 4.2°K field winding area. The unavailability of LN_2 precooling required that the best possible use be made of the boil-off vapors to reduce the conduction leak down this short Dewar wall.

The final configuration of the rotor Dewar is shown in Figure 2. The superconducting field winding is in the section labeled 1. Liquid helium boils off from section 1, and the vapors are funnelled through passages 2 to cool the Dewar walls. Items 3 are hollow bolts used to convey part of the boil-off vapors to the lower end of the Dewar. Items 4 are Styrofoam insulation plugs closing the ends

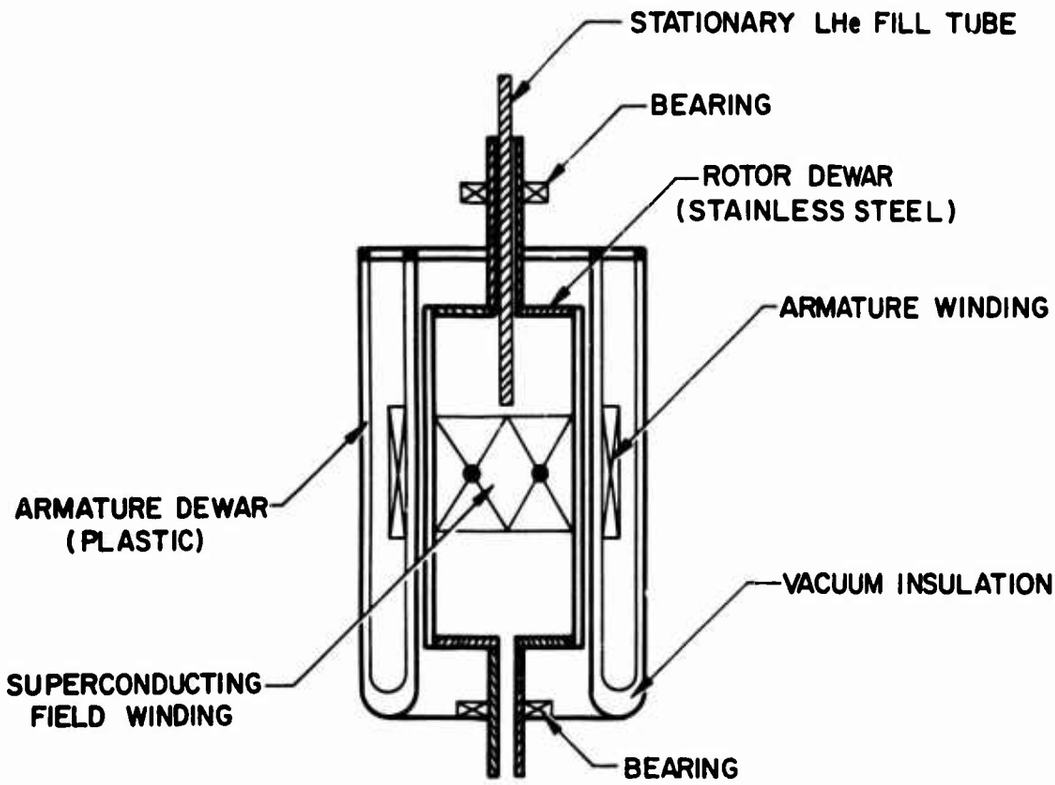

Figure 1. Dewar Arrangement Used in Superconducting Motor.

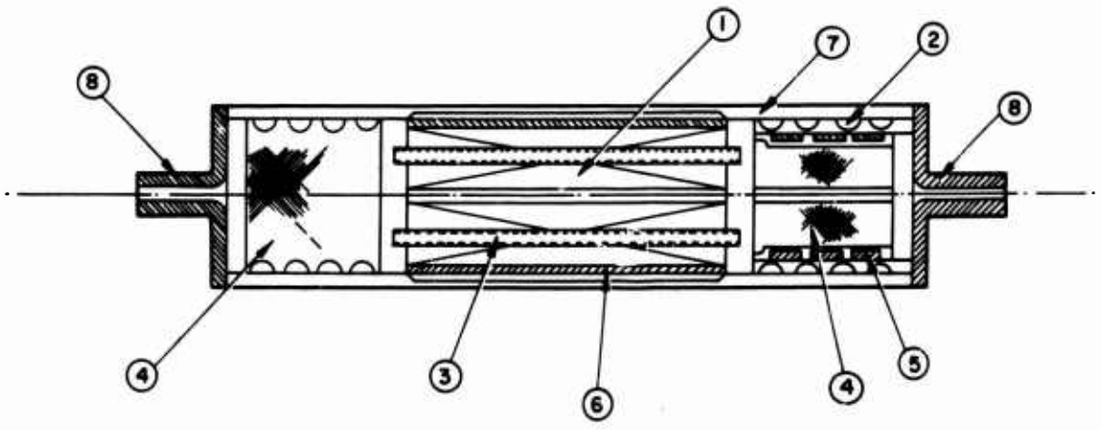

○ : SEE TEXT FOR DESCRIPTION OF ITEMS

Figure 2. Rotor Dewar of Superconducting Motor.

of the Dewar. Part of the vapors used to cool the top end of the Dewar is also diverted to cool the energizing leads (item 5) of the field. These leads are of the vapor-cooled type. Item 6 is the banding necessary to keep the field winding from being destroyed under the combined action of magnetic pressure and centrifugal force. Item 7 is the vacuum insulation space around the cooled region, and items 8 are the hollow shafts that allow the boil-off gas to escape and permit liquid helium to be introduced into the field region.

Except for the fact that its walls were made of plastic, the armature Dewar was of conventional design and construction, complete with LN_2 cooled shields on the outside surface. No LN_2 shield was used in the inside of the annular Dewar to keep the machine's air gap at an absolute minimum.

The superconducting field winding of the machine was designed to have two poles. The poles were not wound individually but were joined together to form a single unit. The whole field winding was constructed from a sandwich of 10 pancake coils wound from standard 300-ampere Nb_3Sn tape slit to 1/4 inch width. This type of construction was chosen because it allowed the maximum amount of conductor to be packed in the space available.

Figure 3 shows the field winding used in the experimental machine. Clearly visible is the sandwich type of construction with the 10 Nb_3Sn pancake coils forming the 10 layers and the vertical cooling passages that carry liquid helium to the core of the winding and to the outside surface of each pancake.

The field winding was inserted into a 3/8-inch-thick stainless steel can, used both as the banding structure and as the liquid helium container. Figure 4 shows the outside of this can, the insulating plug (item 4 of Figure 2), and the spiral vapor-cooled leads (item 5 of Figure 2) attached to the field.

The machine's armature was wound from Nb-60% Ti SG100D superconducting wire. This wire is copper stabilized with an outer diameter of 0.020 inch and a Nb-60% Ti core of 0.011-inch diameter. The copper cladding allows this armature to be operated in the nonsuperconducting mode. In this mode, a modest current can be drawn, consistent with the small amount of copper on the wire. Figure 5 is a schematic diagram of the armature winding form. There are two wires per vertical slot, and each is enclosed in a perforated Teflon sleeve. The holes allow intimate contact between the cooling fluid (LN_2 or LHe) and the wire. The winding form is of linen phenolic and comes apart easily to allow any type of wire to be wound into the armature.

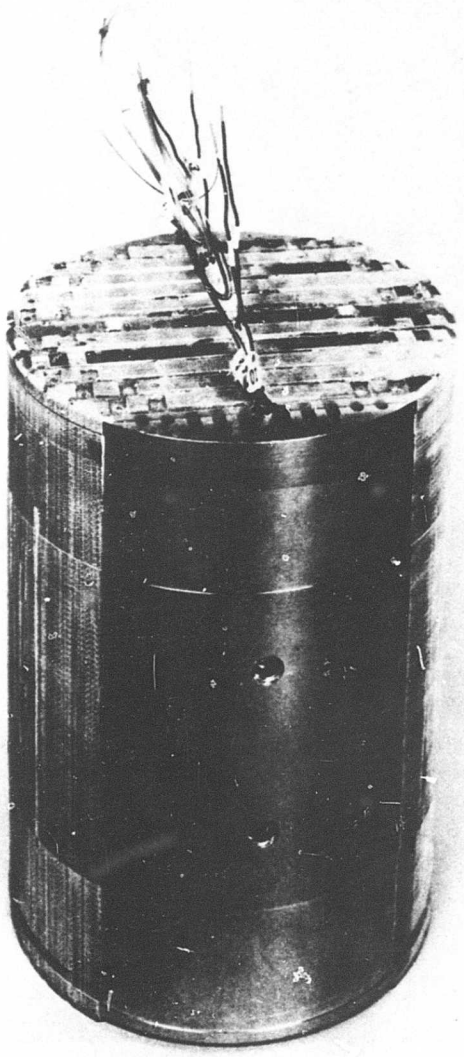

Figure 3. Two-Pole Superconducting Field Winding.

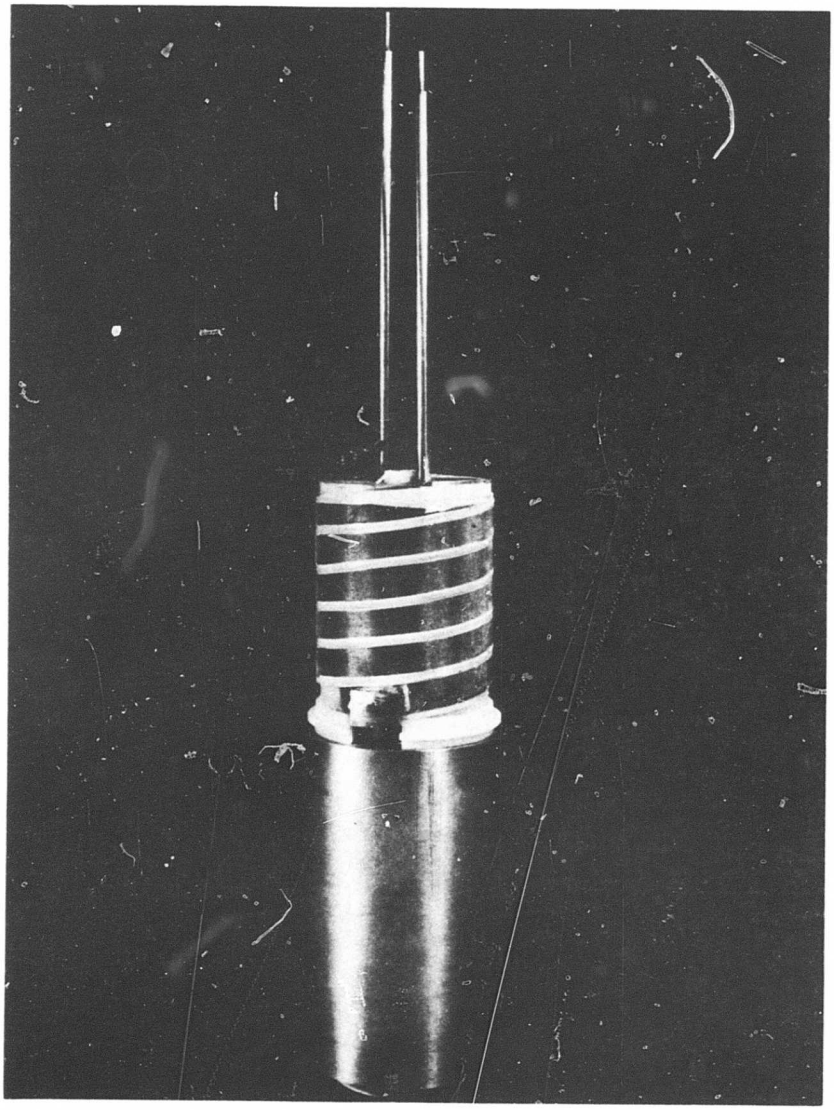

Figure 4. Superconducting Field Winding in Its Banding Container With Attached Vapor-Cooled Leads.

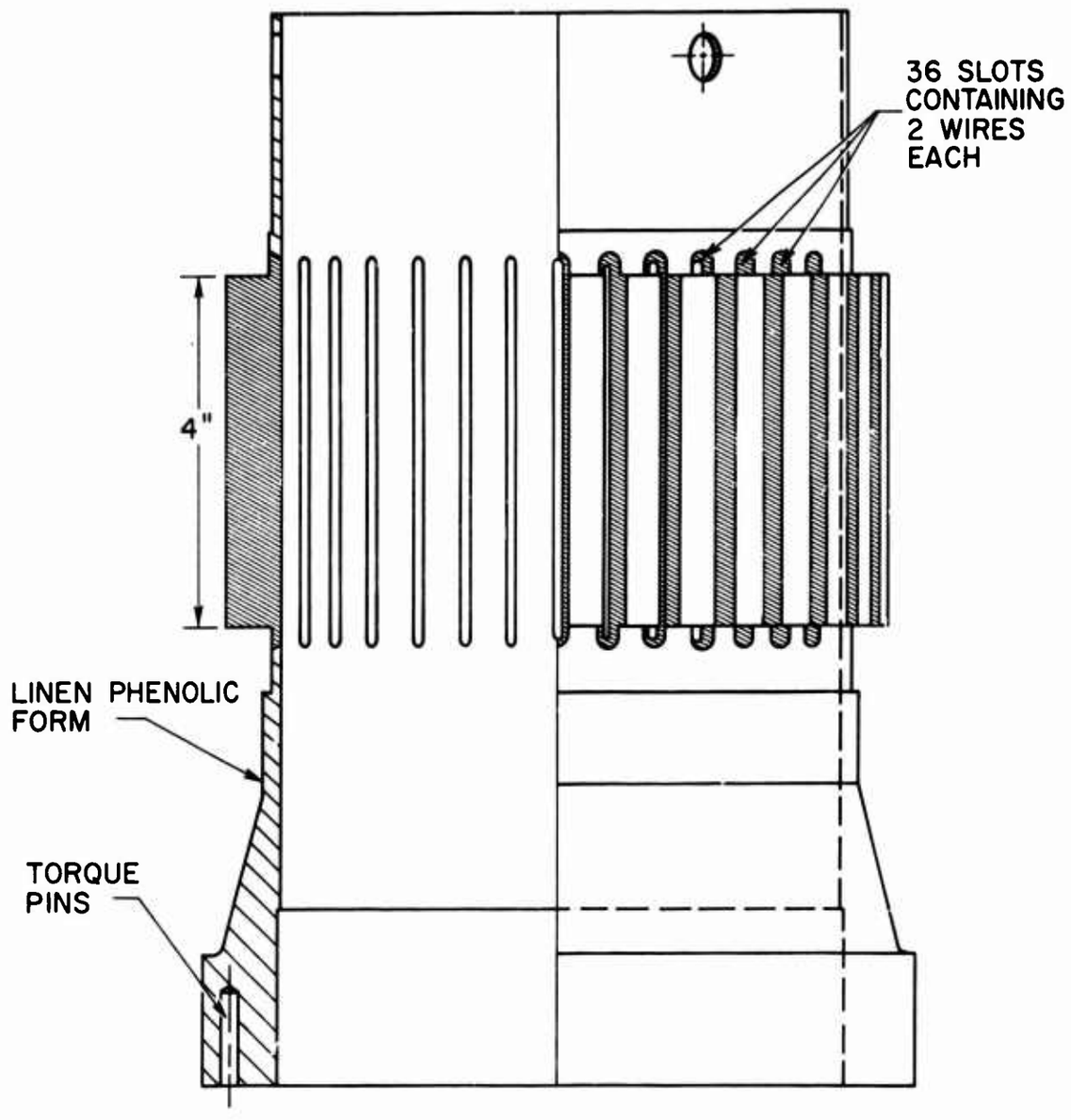

Figure 5. Schematic of Armature Winding Form.

2. Mechanical Design

The machine components must withstand all operational strains and must prevent excessive heat leak to the liquid-helium-cooled regions. The region where these two requirements are most in conflict is the inner wall of the rotor Dewar. This wall is used to transmit torque between the field winding and the end shaft.

This wall must support its own weight, the weight of the plastic end plugs, and that of the copper vapor-cooled leads when these masses are subjected to the high centrifugal acceleration caused by the 12,000-rpm speed of the machine. This last requirement is by far the most severe and is, therefore, the one that determines the minimum wall thickness. The forces caused by centrifugal acceleration plus the pressure differential of the vacuum space combine to impose a pressure of 3.52×10^2 lb/in.^{2} on the Dewar wall in question. For a Dewar with a bore radius of 2.55 inches and a 0.032-inch-thick wall, this is equivalent to a hoop tension stress of 28,000 lb/in.^{2} at 12,000 rpm. As the yield strength of Stainless Steel - 304 is of the order of 35,000 psi, the wall thickness could not be safely reduced beyond this 0.032-inch value and the heat leaks from this wall thickness have to be accepted.

The outside wall of the Dewar transmits no torque between field winding and end shafts. Its main mechanical function is to keep the end flanges of the Dewar parallel. Since the wall does not contribute to the heat leaks, its thickness was set at 0.050 inch.

As was pointed out in Section II. A. 1, the Dewar necks had to be shorter than cryogenic consideration would dictate to keep the critical frequency of the rotor higher than 200 cps. To estimate the first critical frequency of the Dewar, the rotor was assumed to be made up of 3 large weights (the field flanked by the two end shafts) joined by lengths of shafts (the Dewar walls on each side of the field).

The natural frequency[6] of shafts carrying several weights is

$$\frac{1}{w_c^2} = \frac{1}{w_o^2} + \frac{1}{w_1^2} + \frac{1}{w_2^2} + \cdots$$

where w_c = critical speed of entire shaft assembly

w_o = critical speed of shaft only

w_1 = critical speed of shaft carrying only w_1

w_2 = critical speed of shaft carrying only w_2

Following this analysis, we arrive at a critical speed of

$$w_c = 21,500 \text{ rpm}$$

which leaves us ample leeway at an operational speed of 12,000 rpm.

The Nb_3Sn ribbon used to wind the superconducting field possesses little mechanical strength. The magnetic and centrifugal forces on it had to be supported by a banding structure. To design this, the banding is assumed to be a cylinder containing a rotating fluid (the superconducting winding) whose density is equal to that of Nb_3Sn tape. If one calculates the pressure such a rotating fluid would impose on the cylinder walls that contain it, one arrives at the expression

$$\frac{F}{A} = \frac{\rho R}{2} + \frac{4\pi^2 f^2 \rho R^2}{3g}$$

$$= \text{gravitational force} + \text{centrifugal force}$$

where R = radius of field winding

ρ = density of field winding

f = rotational speed (cps)

If a 20% overspeed on the machine (ω = 240 cps) is assumed, the pressure exerted by the unsupported field winding on its banding container is

$$\frac{F}{A} = 3460 \text{ psi}$$

To this force must be added the force due to magnetic pressure, which could be as high as 1400 psi. The field OD and Dewar ID left enough room for approximately 18 layers of 10 mil type 302 stainless steel wire to be wound around the field structure. The resultant stress in such a banding would be 70,000 psi. The full hard SS wire tested at over 300,000 psi tensile. However, the process of applying 18 layers of this wire to the field structure proved to be so time consuming in its early stages that it was abandoned (at some sacrifice in top rotational speed) for a single, type 304 SS tube that was sweated over the field winding. The OD of the SS tube was then machined to give a snug fit inside the Dewar. This reduced the top speed to around 9600 rpm, based on a comparison of allowed safe stress.

The machine was constructed to operate vertically, which greatly simplified the problem of feeding liquid helium to the field winding. In this configuration, one can rely on gravity and centrifugal forces

to get the coolant to all parts of the field winding. A horizontal design would need a pressurized coolant system to assure proper cooling of the field at all rotational speeds (including stationary).

The bearings for the machine presented a special problem. As explained in the previous section, the boil-off gas from the field winding space is used to cool the walls of the rotor Dewar. During cool-down operations (which last a few hours), the boil-off is quite large and the amount of refrigeration available in the bearing region is appreciable. This caused the bearings to run much colder than anticipated and eventually to seize. This problem was circumvented by wrapping an electric heater around the housing of the top bearing and by blowing hot nitrogen gas directly onto the shaft above the bottom bearing. These remedies have succeeded in maintaining the bearings at approximately room temperature.

3. Electrical Design

a. Field Winding

The design for the superconducting field of the machine was a compromise between conflicting requirements. Proper cooling requires that the coil have an open geometry to contain passages for the liquid helium. On the other hand, the large centrifugal forces involved in this application dictated that the coil windings be closely packed so that each layer of wire supported its neighbor.

It was decided to use Nb_3Sn unstabilized tape to wind the pancakes because of the higher critical temperature of Nb_3Sn as opposed to Nb-Ti and because the copper needed to stabilize the superconductor would have reduced the allowable current density below what was believed to be an acceptable level. Commercially available Nb_3Sn tape used without any backing is mechanically weak and must rely on support structures to withstand the magnetic and centrifugal operational loads. Because of this inherent mechanical weakness and because of the large magnetic and centrifugal loads imposed on the winding, it was decided to design a mechanically strong structure at the expense of some cooling qualities.

The Nb_3Sn pancakes were rigidly supported between layers of plastic laminate (G-10). Liquid-helium cooling was provided on the ID and OD of each pancake. The center of the winding relied on conduction cooling to maintain superconductivity.

It was not expected that such a winding would allow the superconductors to carry current up to full H-I curve value of the conductor, but

the small size of the field winding and the stringent mechanical requirements made this type of construction mandatory.

b. Armature Winding

The rms voltage per phase for an armature is given by Reference 7:

$$E_{rms} = 4.44\, k_b\, k_p\, f\, N_{ph}\, \phi \text{ volts/phase}$$

where k_b = breadth factor of the winding

k_p = pitch factor of the winding

f = frequency c/s

N_{ph} = number of turns per phase

ϕ = fundamental harmonic of flux per pole.

To minimize the harmonic content of both the voltage and the mmf waves, a distributed, fractional-pitch armature winding with 5/6 pitch was chosen. The armature is a double-layered, three-phase, two-pole winding with a total of 36 slots. For such a winding, the distribution factors for the fundamental are

$$k_b = \frac{\sin(n\gamma/2)}{n \sin(\gamma/2)} = 0.958$$

$$k_p = \cos\frac{\Pi - 150^\circ}{2} = 0.96$$

Hence, for the fundamental $\left(k_p\, k_b\right) = 0.92$.

For the 5^{th} and 7^{th} harmonics, these factors are

5^{th} harmonic $\left(k_p\, k_b\right) = 0.05$

7^{th} harmonic $\left(k_p\, k_b\right) = 0.03$

We see that the fundamental is relatively unattenuated whereas the undesirable harmonics are greatly reduced by this winding. The output voltage of this armature as a function of frequency and field flux at the armature is plotted in Figure 6.

The machine is designed to produce about 15 hp at the operational speed of the motor (12,000 rpm). From Figure 6 we see that at a 200 c/s, and at an excitation field of about 5 kg, the open-circuit armature-induced voltage is 70 volts, line to neutral. To produce the required 15 hp (11,200 watts), the Y-connected 3ϕ armature must carry 54 amps.

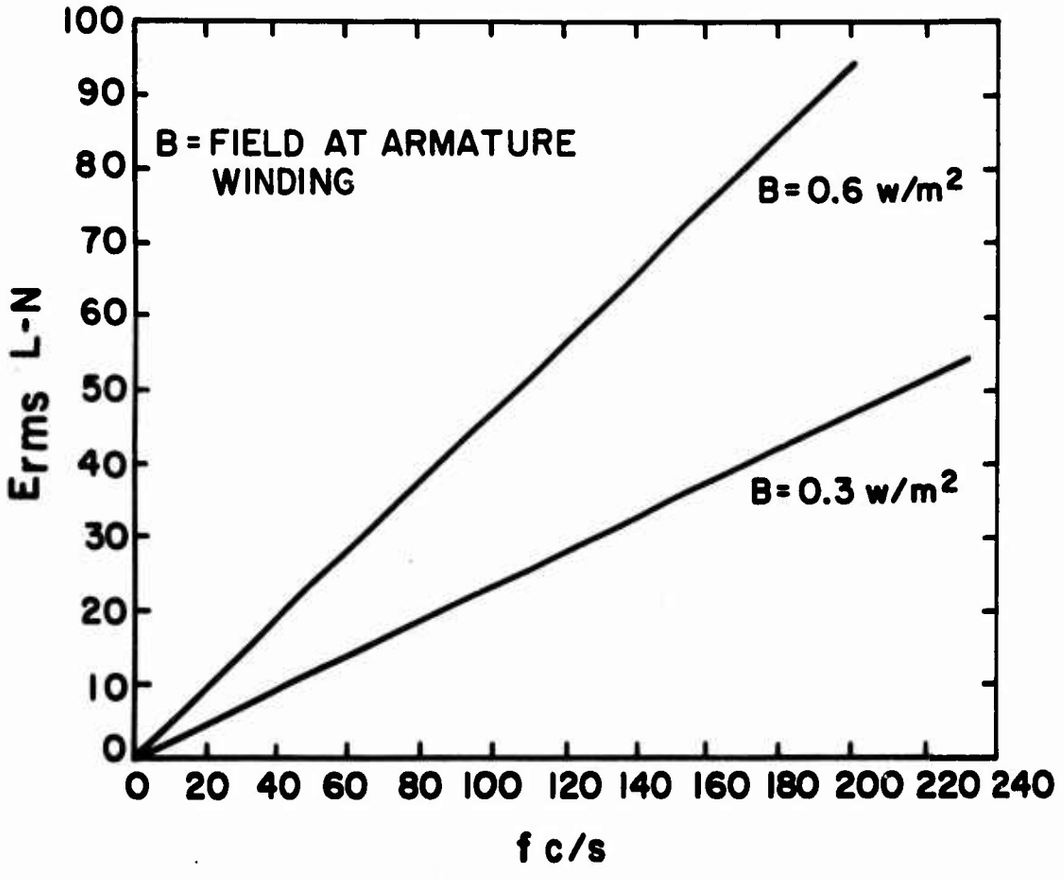

Figure 6. Prediction of Armature Output Voltage Versus Frequency.

Figure 7 is a plot of the H-I curve for the superconductor used in the armature winding. At 5 kg this wire will carry over 150 amperes. The armature should therefore be able to produce the required 15 hp in its superconducting state.

c. Prediction of Machine Performance

Large synchronous machines with superconducting field winding were analyzed at Avco.[8] Table I lists the design formulas linking the electric parameters with the dimensions of the various machines. Table II defines the symbols used in Table I, and Figure 8 defines the geometry used in the machine analysis. Table III lists the various nondimensional parameters and geometric dimensions that are applicable for the superconducting machine. Table IV lists the calculated values of the mutual inductances, and phase voltage as computed from Table I. These calculated values will be compared with the measured values of Section II. C.

d. Superconducting Armature in Sweeping AC Field

The losses developed in a superconducting armature in the presence of a sweeping AC field are now evaluated. In a later section, they will be compared with measurements obtained for this armature. No other data or theoretical prediction is available for comparison. The eddy current losses in the copper of conventional armature can also be predicted. From these two sources of information, it is possible to obtain an order-of-magnitude approximation concerning the losses that are experienced by the superconducting armature.

Using the experimental results of Reference 5, we can predict hysteresis loss in the superconducting wire of the armature. It is expected from Reference 9 that this loss will be 3 or 4 times smaller than that occurring in the sweeping field case. It will nevertheless serve as a guideline for what is to be expected.

Figure 9 is a plot of the expected loss predicted for a bare 10-mil-diameter superconducting wire subjected to a stationary sinusoidally varying field.[5] To this loss we must add the eddy current loss in the copper cladding of the superconductor.

For a sinusoidally varying B field, the eddy current loss in copper is derived in the appendix as

$$\text{Losses} = 1.173 \times 10^{-4} f^2 B^2$$

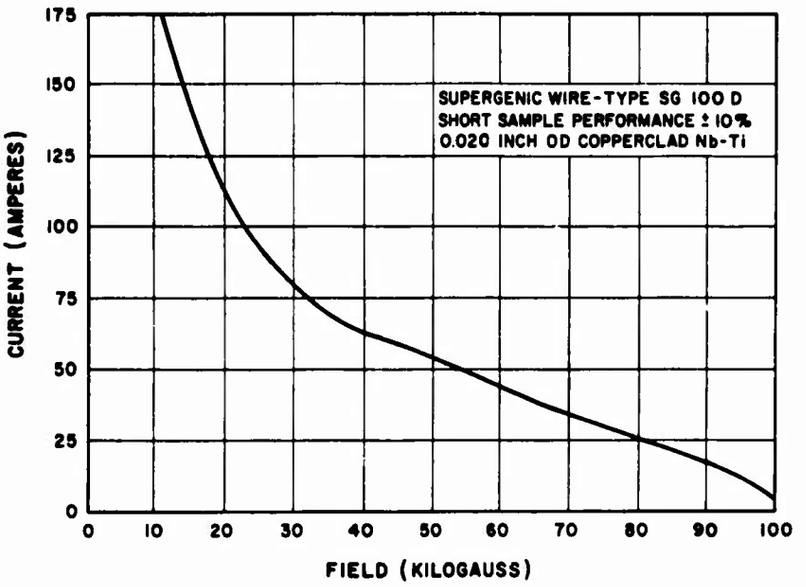

Figure 7. H-I Characteristic of Wire Used to Wind the Armature.

TABLE I. SUMMARY OF DESIGN EQUATIONS FOR A SHIELDED SYNCHRONOUS MACHINE

Parameter	No. of Pole Pairs $p \neq 2$	$p = 2$
M Mutual Inductance Armature-Field	$\frac{48\mu_o N_a N_f \ell_T}{\pi^3 p (1-x^2)(1-y^2)} (x-\delta)^p (1-y^{p+2}) \left[\frac{(1-x^{-p+2})}{(4-r^2)} + \frac{(1-x^{p+2})}{(2+p)^2}\right]$	$\frac{6\mu_o N_a N_f \ell_T (1+y^2)(x-\delta)^2}{\pi^3 (1-x^2)} \left[\ell n \frac{1}{x} + \frac{1}{4}(1-x^4)\right]$
R_a Armature Resistance per phase	$\frac{12 N_a^2 \rho_a x^2 \left[\frac{\ell}{R_i} + \frac{\pi}{2p}\left(\frac{1+x}{x}\right)\right]}{\pi \lambda_a R_i (1-x^2)}$	Same as for $p \neq 2$
L_a Armature Inductance	$\frac{36\mu_o N_a^2 \ell_T}{\pi^3 p (1-x^2)^2} \left[\frac{(p-2)-(p+2)x^4+4x^{p+2}}{(p^2-4)} + 2\frac{(1-x^{p+2})^2}{(p+2)^2}\right]$	$\frac{9\mu_o N_a^2 \ell_T}{2\pi^3 (1-x^2)^2} \left[(1-x^4) + x^4 \ell n x + \frac{1}{2}(1-x^4)^2\right]$
L_f Field Inductance	$\frac{16\mu_o N_f^2 \ell_T}{\pi^3 p (1-y^2)^2} \left[\frac{(p-2)-(p+2)y^4+4y^{p+2}}{(p^2-4)} + 2(x-\delta)^{2p}\frac{(1-y^{p+2})^2}{(p+2)^2}\right]$	$\frac{2\mu_o N_f^2 \ell_T}{\pi (1-y^2)^2} \left[(1-y^4) + y^4 \ell n y + \frac{1}{2}(x-\delta)^4 (1-y^4)^2\right]$
P Power	$\frac{6}{\quad} \omega_m \mu_o J_a J_f R^5 (1-y^{p+2})(x-\delta)^{p+2} \left[\frac{\ell_T}{\quad} - \frac{\pi}{\quad}(1+x)\right] \left[\frac{(1-x^{-p+2})}{\quad} + \frac{(1-x^{p+2})}{\quad}\right] \cos\theta$	$\frac{3}{\quad} \omega_m \mu_o J_a J_f R_o^5 (1-y^4)(x-\delta)^4 \left[\frac{\ell_T}{\quad} - \frac{\pi}{\quad}(1+x)\right] \left[\ell n \frac{1}{\quad} + \frac{1}{\quad}(1-x^4)\right]$

	[illegible]	[illegible]
$R_s - R_o$ Shield Thickness	$\frac{4\mu_o J_f R_o (x-\delta)^{p+2}(1-y^{p+2})}{\pi B_a p(p+2)}$	Same as for $p \neq 2$
x_s Normalized Synchronous Reactance	$\frac{J_a \frac{\ell_T}{R_o}\left[\frac{(p-2)-(p+2)x^4+4x^{p+2}}{(p^2-4)}+2\frac{(1-x^{p+2})^2}{(p+2)^2}\right]}{4J_f\left[\frac{\ell_T}{R_o}-\frac{\pi}{3p}(1+x)\right](x-\delta)^{p+2}(1-y^{p+2})\left[\frac{(1-x^{-p+2})}{(4-p^2)}+\frac{(1-x^{p+2})}{(p+2)^2}\right]}$	$\frac{J_a \frac{\ell_T}{R_o}\left[\frac{1}{4}(1-x^4)+x^4 \ln x+\frac{1}{8}(1-x^4)^2\right]}{J_f\left[\frac{\ell_T}{R_o}-\frac{\pi}{6}(1+x)\right](x-\delta)^4(1-y^4)\left[\ln\frac{1}{x}+\frac{1}{4}(1-x^4)\right]}$
$\frac{I_a R_a}{V_a}$ Normalized Joule Loss	$\frac{2.24 J_a \rho_a (1+x)(1-x^2)}{16\lambda_a \omega_m \mu_o J_f R_o^2 (1-y^{p+2})(x-\delta)^{p+2}\left[\frac{(1-x^{-p+2})}{(4-p^2)}+\frac{(1-x^{p+2})}{(p+2)^2}\right]}$	$\frac{2.24 J_a \rho_a (1+x)(1-x^2)}{64\lambda_a \omega_m \mu_o J_f R_o^2 (1-y^4)(x-\delta)^4\left[\ln\frac{1}{x}+\frac{1}{4}(1-x^4)\right]}$
V_a/N_a Volts Per Turn	$\frac{24\omega_m \mu_o J_f R_o^2 \ell_T (x-\delta)^{p+2}(1-y^{p+2})}{(1-x^2)}\left[\frac{(1-x^{p+2})}{(4-p^2)}+\frac{(1-x^{p+2})}{(2+p)^2}\right]$	$\frac{6\omega_m \mu_o J_f R_o^2 \ell_T (x-\delta)^4(1-y^4)}{(1-x^2)}\left[\ln\frac{1}{x}+\frac{1}{4}(1-x^4)\right]$
E_f Normalized Field Energy	$\frac{2\mu_o J_f^2 R_o^4 \ell_T (x-\delta)^4}{\pi p}\left[\frac{(p-2)-(p+2)y^4+4y^{p+2}}{(p^2-4)}+2(x-\delta)^{2p}\frac{(1-y^{p+2})^2}{(p+2)^2}\right]$	$\frac{\mu_o J_f^2 R_o^4 \ell_T (x-\delta)^4}{4\pi}\left[(1-y^4)+y^4 \ln y+\frac{1}{2}(x-\delta)^4(1-y^4)^2\right]$

TABLE II. NOMENCLATURE FOR TABLE I

B_f	=	magnitude of flux density produced by field current alone
B_s	=	saturation value of flux density in the iron shield
I_a	=	amplitude of armature phase current
I_f	=	field terminal current
J_a	=	amplitude of effective armature winding current density, including the effect of space factor due to cooling, insulation, and structure
J_f	=	effective field winding current density, including the effect of space factor due to cooling, insulation, and structure
L_a	=	armature self-inductance per phase
ℓ_T	=	overall length of machine
M	=	maximum value of space fundamental component of mutual inductance between field winding and one armature phase
N_a	=	total number of series turns per phase on armature winding
N_f	=	total number of series turns on field winding
p	=	number of pairs of poles
pf	=	cos Θ = load power factor
P	=	generator power output
R_a	=	armature resistance per phase
R_1	=	inside radius of field winding
R_2	=	outside radius of field winding
R_i	=	inside radius of armature winding
R_o	=	outside radius of armature winding
R_s	=	outside radius of iron shield
x	=	R_i/R_o
χ_a	=	per unit armature synchronous reactance
y	=	R_1/R_2
ν	=	volume
V_a	=	amplitude of armature phase to neutral voltage
Δ	=	air gap width
δ	=	normalized air gap width = $\frac{\Delta}{R_o}$
λ_a	=	armature packing factor
ρ_a	=	resistivity of armature conductor
ω	=	armature electrical frequency
ω_m	=	ω/p machine shaft speed

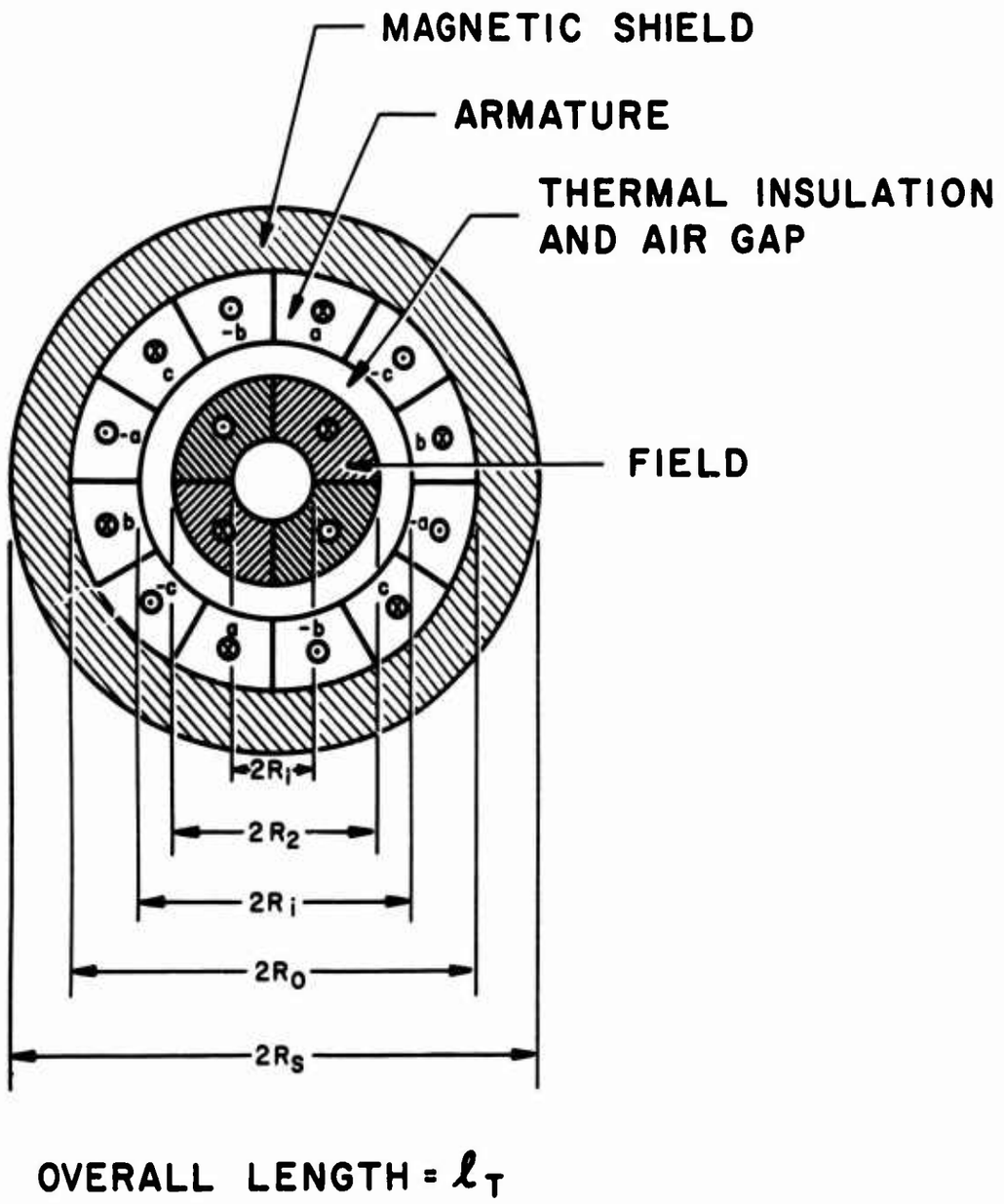

Figure 8. Configuration of Synchronous Machine With Magnetic Shield.

TABLE III. GEOMETRIC PARAMETERS OF SYNCHRONOUS ALTERNATOR

$X = \frac{R_i}{R_o} = 0.98$	$R_1 = 0.01$	
$Y = \frac{R_1}{R_2} = 0.1775$	$R_2 = 0.0571$	
$\delta = \frac{\Delta}{R_o} = 0.328$	$R_i = 0.0859$	
$\ell_T = 0.1016$ m	$R_o = 0.0876$	
$N_A = 12$	$\Delta = 0.288$	
$N_f = 3368$	Inside radius or iron shield = 0.140	

TABLE IV. CALCULATED PARAMETERS OF SYNCHRONOUS ALTERNATORS

$M = 1.17$ millihenry

V_a (peak) = 74 volts

V_a (rms) = 52.3

for $N_a = 12$, $I_f = 100$A, $\omega = 100$c/s

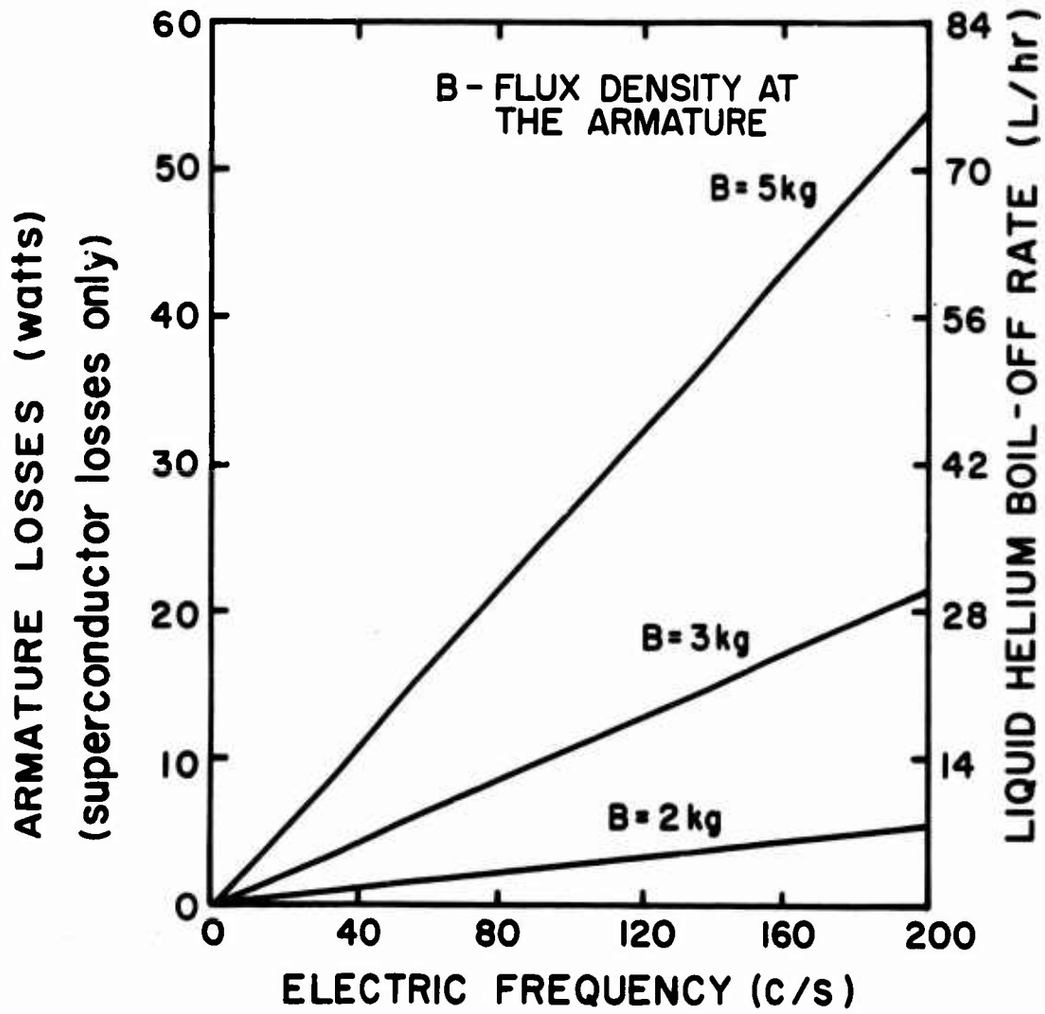

Figure 9. Superconductor Losses Versus Peak Applied Field for the Superconducting Armature.

where

f = frequency of applied field

B = intensity of the applied magnetic field at the armature.

Figure 10 is a plot of the armature eddy current loss for various values of B and f. The sum of these two separate losses is plotted in Figure 11 as a function of frequency and magnetic field intensity. Unless these calculated values of the total losses in the superconducting armature should prove by test to be much lower in magnitude, it will be evident that superconducting armatures are impractical in machines designed for continuous operation.

B. TEST RIG

The superconducting machine was to be tested both as a generator and as a motor over its full operating speed range. The test rig was designed to produce or absorb the 15-hp rating of the superconducting machine over its full range of speed. Figure 12 is a schematic representation of the test apparatus.

In the motor tests, the variable-frequency power supply was hooked up to the superconducting motor armature, and the motor output was measured from the output of the drive/load motor which then acted as a DC generator. To the output of the DC machine must be added the power necessary to overcome windage, brush, and belt drive drag. These have been measured and are plotted in Figure 13. This same drive/load motor was used to start the synchronous superconducting machine in the regular fashion.

In generator tests, the drive/load DC machine was used to drive the superconducting machine as a generator. The output from the machine's armature (both normal and superconducting) was fed to a unity power factor load and measured.

The heat leak and eddy losses in the superconducting armature were measured by channeling the boil-off from the helium Dewar through a calibrated flow meter.

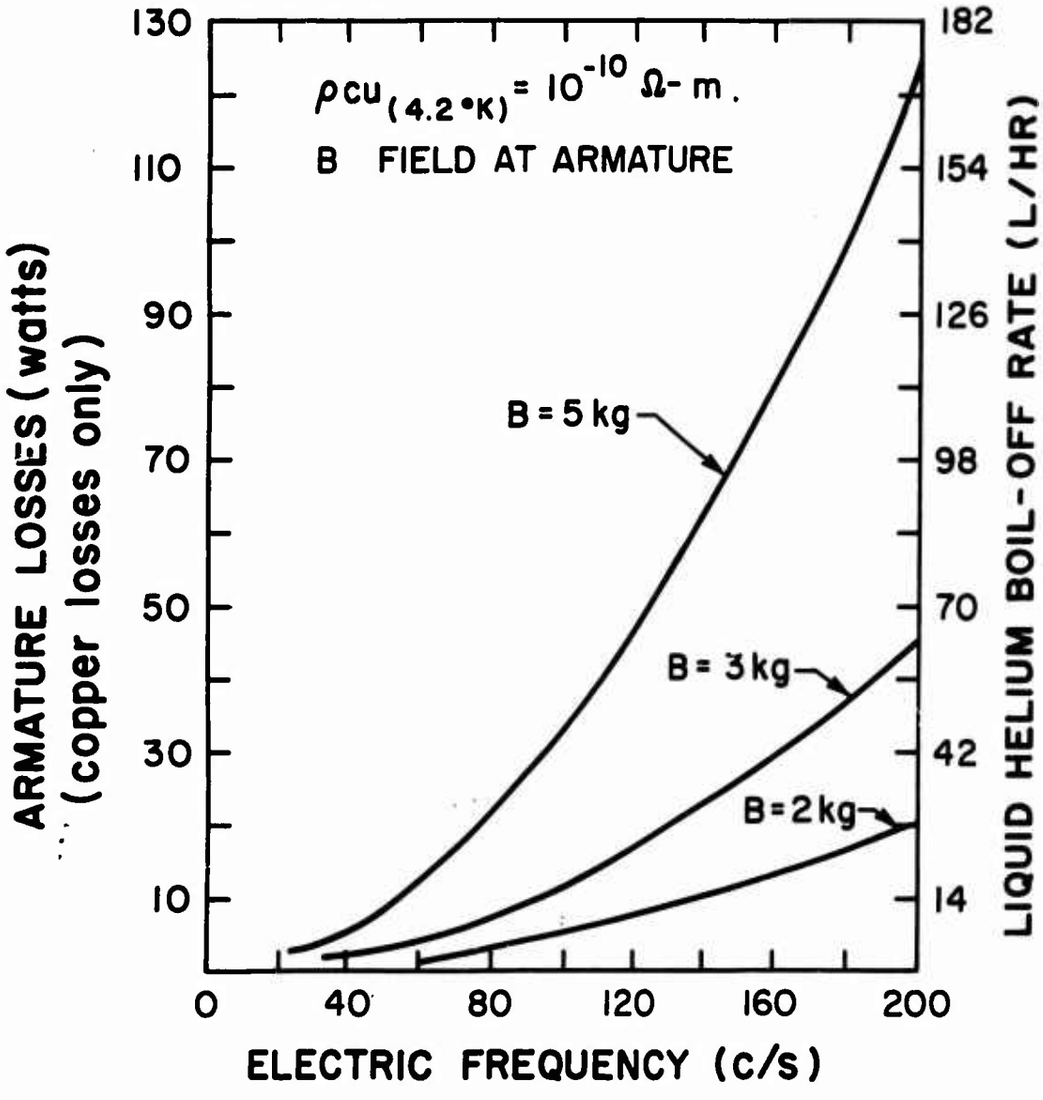

Figure 10. Copper Losses Versus Peak Applied Field for the Superconducting Armature.

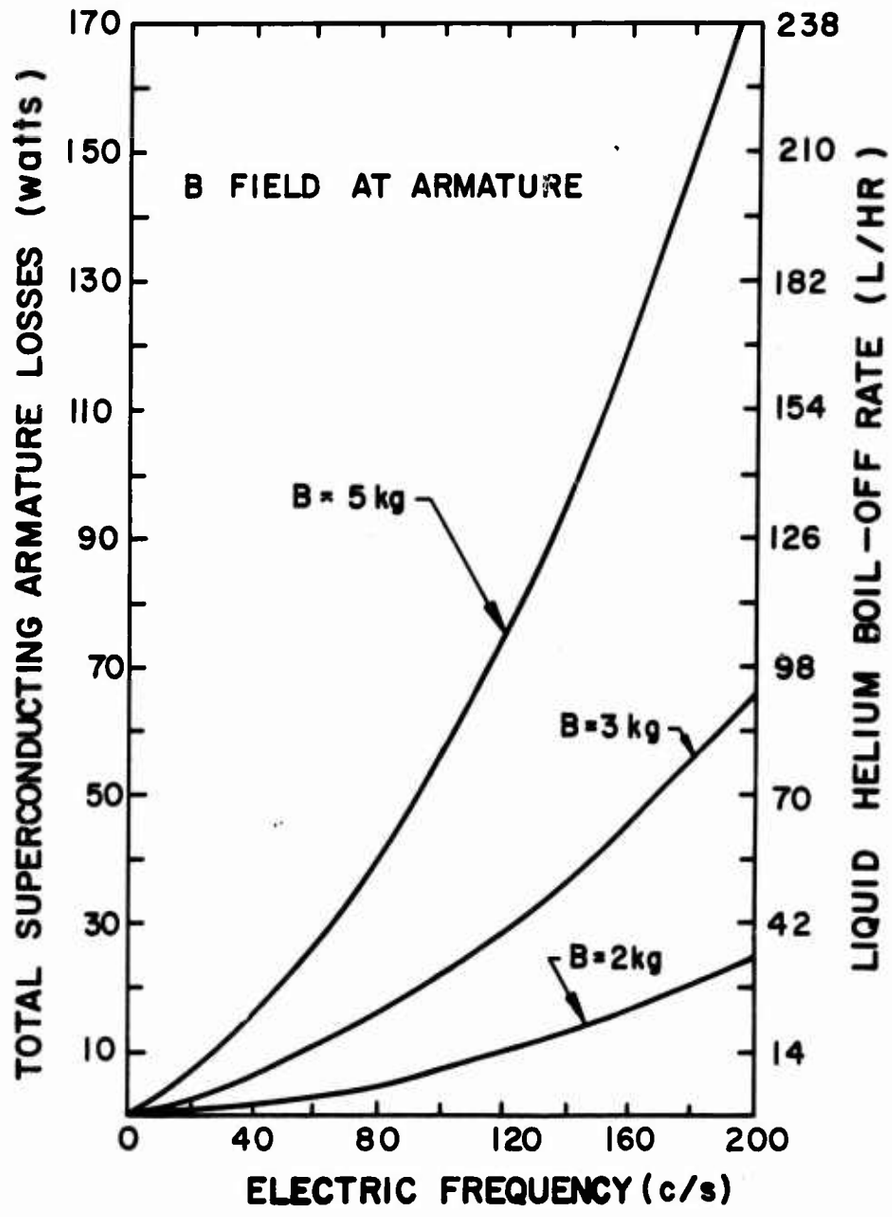

Figure 11. Total Armature Losses Versus Peak Applied Field.

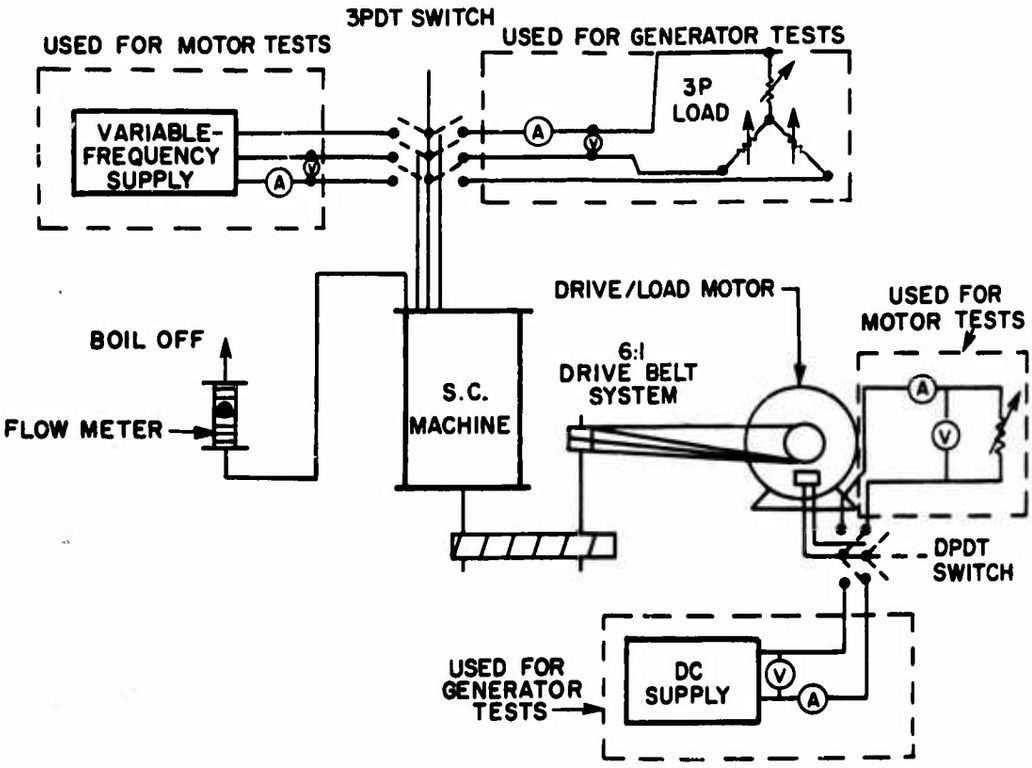

Figure 12. Schematic of Test Arrangement.

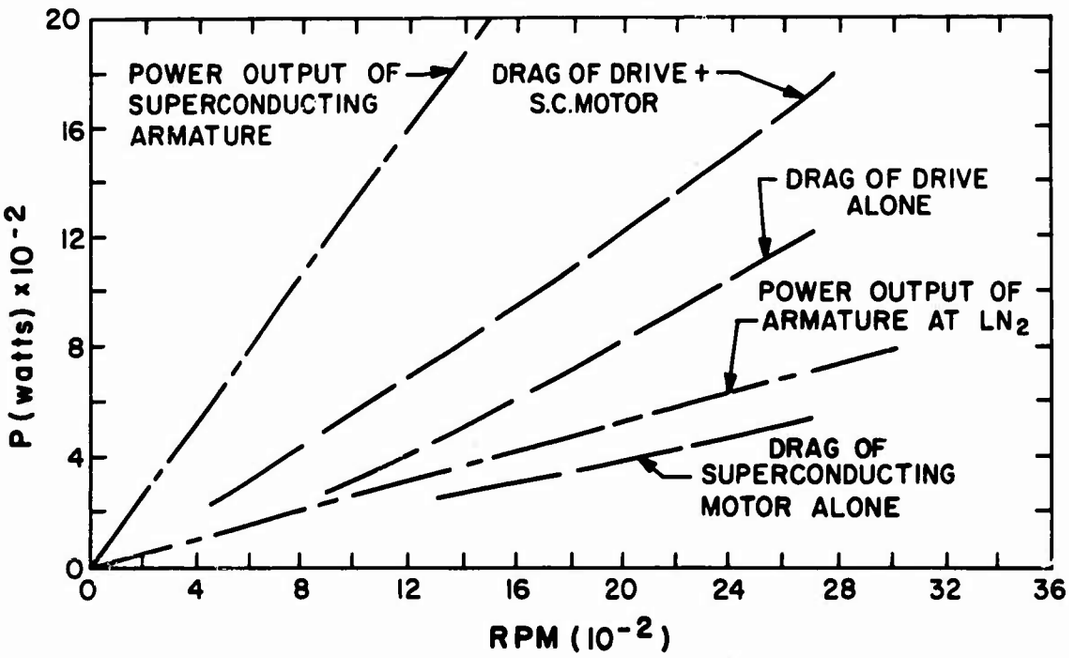

Figure 13. Power Out of Armature and Drag of Drive System Versus RPM.

C. EXPERIMENTAL RESULTS

1. Field Winding

The field winding was constructed following the design philosophy described in Section II. A. Figure 3 is a photograph of the assembled field winding clearly showing the sandwich construction with the 10 Nb_3Sn pancakes. Also visible on the photograph are the vertical cooling passages that allow the helium to be carried to the center of the winding and the stainless steel supports located at the poles. Figure 4 shows the field winding in its stainless steel banding cylinder complete with the assembled, spiraled, vapor-cooled leads. The banding structure also serves as the liquid helium container for the superconducting field.

Once assembled, the field winding was suspended in a large laboratory Dewar and cooled to liquid helium temperature. Five calibrated magnetoresistive probes had been attached to the surface of the field banding. Their location is as depicted in Figure 14. One probe is on the field axis and one on each side at 30° and at 45° from the field axis reference line.

The field winding was found to quench at 120 amperes. This is about 60% of the H-I curve and is considered to be reasonable when one takes into account the mechanical limitations imposed on the cryogenic design.

The real measure of the quality of the current achieved in this field winding becomes evident when the current density of this field winding is compared with that of conventional machines. The current density in the field winding is given by

$$J_f = \frac{2 I_f N_f}{\pi (R_2^2 - R_1^2)}$$

where the symbols are as defined in Table II. For the 120-ampere quenching current, this comes to

$$J_f = 6.2 \times 10^3 \ A/cm^2$$

This is at least an order of magnitude larger than the current densities available in room-temperature windings. A polar plot of the field intensity at the surface of the field winding as a function of field excitation is given in Figure 15.

The heat leak to the field winding was measured by channeling the liquid helium boil-off through a flow meter. The heat leak was measured to be 12 watts (17 L/hr LHe). This is about twice the size of the

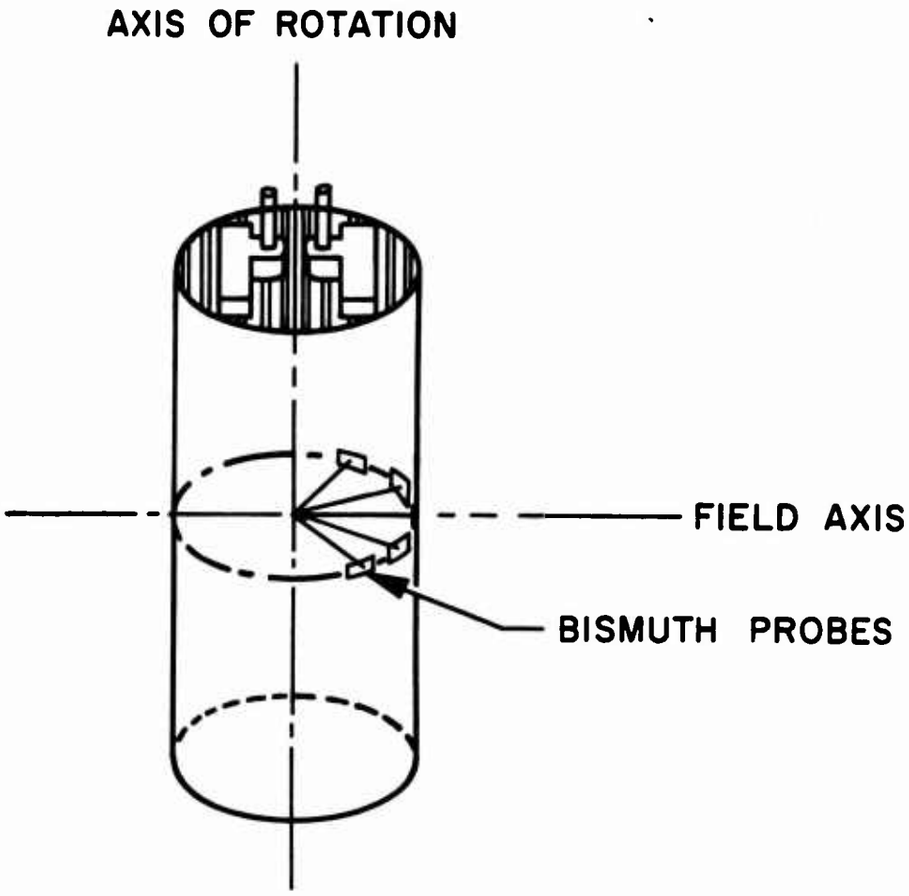

Figure 14. Location of Field Probes on Superconducting Field Winding.

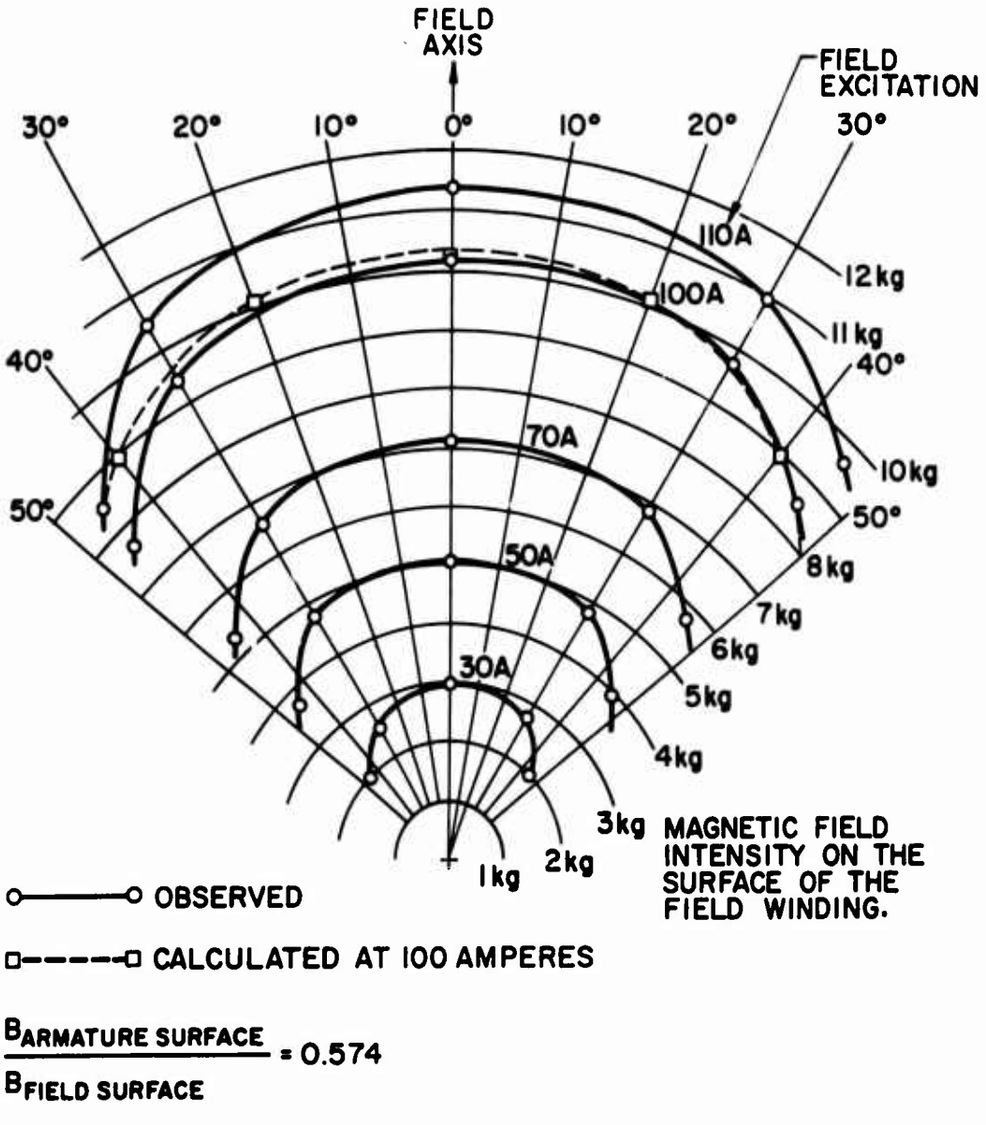

Figure 15. Radial Plot of Field Intensity as a Function of Field Excitation.

estimated heat leak (6.5 watts). This discrepancy was realized because (1) the Dewar could not be evacuated to the expected degree and (2) all heat leak calculations were based on the full usage of the boil-off vapors to cool the Dewar walls and the vapor-cooled leads, but the many escape parallel paths available to the helium boil-off gas prevented its full use as a regenerative cooling agent.

2. Generator Tests

As a necessary preliminary step to the motor test, generator tests were carried out in the superconducting machine.

As stated in Section II.A.2, some problems due to excessive cooling of the bearings were encountered in the preliminary tests. The very cold temperatures to which the bearings were subjected caused the top bearing to seize. This stopped the rotor and resulted in the full overload torque of the drive motor (20 hp) being applied suddenly to the rotor half shafts. This large unforeseen torque caused both half shafts to be bent enough to prevent operation at rotational speeds above 3000 rpm. All subsequent tests were therefore limited to the 0-3000 rpm range.

The following cool-down procedure was used for each test. The field winding was first cooled and made superconducting. After this was achieved, the armature winding was cooled to liquid nitrogen temperature and data were taken with the armature cooled in this fashion. The test apparatus was then adjusted at a minimum cost in liquid helium (only the field was superconducting). Then the armature was cooled to liquid helium temperature and made superconducting, and data were taken.

Because these tests were the first ones ever run on the machine, much time (and liquid helium) was expended before the armature could be cooled to LHe temperatures, and the amount of liquid helium available then was too small to allow full testing of the armature in the superconducting configuration. Most of the data were therefore obtained with the field superconducting but with the armature at LN_2 temperatures.

The open-circuit characteristics of the machine with its armature in LN_2 and liquid helium were measured at different speeds. The results are shown in Figure 16, where the open-circuit line-to-line output voltage is plotted as a function of both field excitation and rotational speed. From these results it is possible to estimate the accuracy of the formulas derived in Reference 8, especially for the construction of superconducting rotating electric machinery.

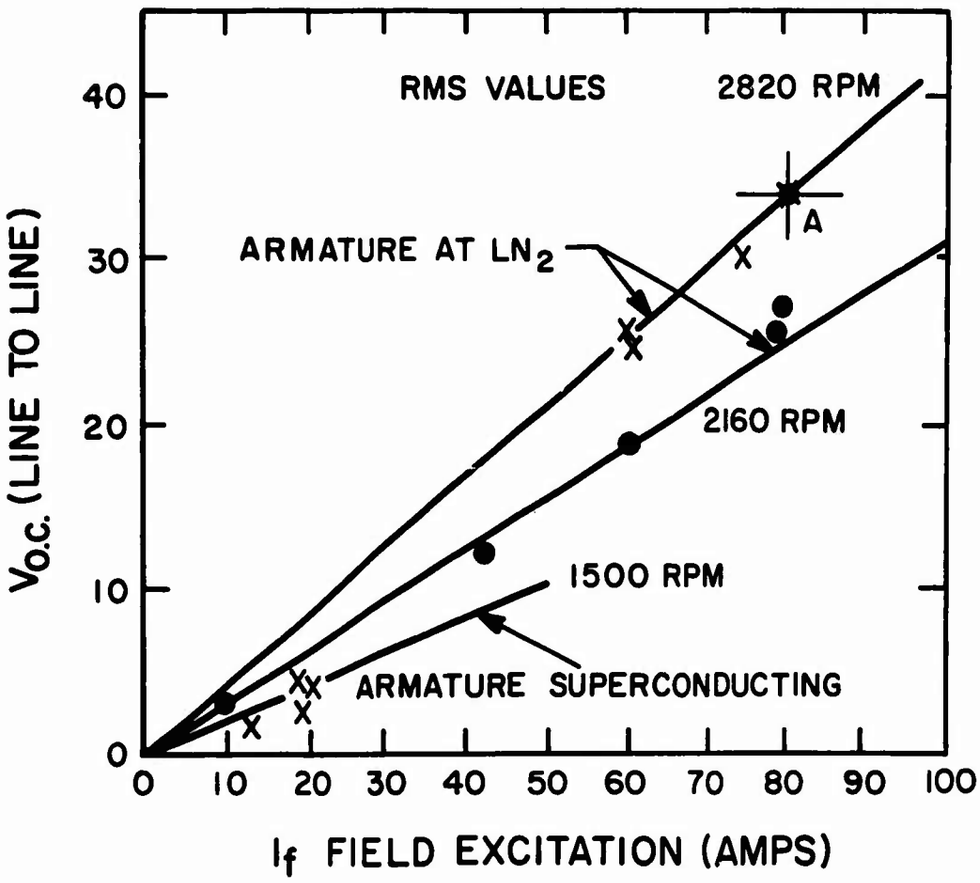

Figure 16. Open-Circuit Characteristics Versus Field Excitation.

The mutual inductance of the two windings is given by the relationship

$$M = \frac{V_a}{\omega I_f}$$

where

V_a = amplitude of the phase voltage

ω = armature electrical frequency

I_f = field excitation current

Table V compares the predicted values of Section II. A. 3 with the values measured in the experimental run. The agreement in the values of the mutual inductance M and phase voltage V_a coincides well within the experimental error.

Once the open-circuit characteristics of the machine were measured, the armature of the superconducting machine was connected to a unity power factor load, and the terminal characteristics of the machine were recorded as shown in Figure 17. This figure shows the relationship between the output voltage and the output current for various speeds, field excitation, and temperature of the armature. These quantities are self-consistent within a few percent, which is well within the experimental error. The current drawn from the armature was purposely kept to a low value to avoid damaging the armature. Less data were obtained with the armature at liquid helium than with the armature at liquid nitrogen temperature for the reasons stated above. Nevertheless, the helium temperature data are consistent with the predictions of Section II. A. 3.

A single point was obtained for the armature losses in the superconducting state. The declining supply of liquid helium at the time that these data were taken did not allow a wait for thermal equilibrium. Therefore, the boil-off of liquid helium due to armature losses had to be obtained from an uncertain background.

The result was obtained at a field excitation current of 16 amperes and a rotational speed of 1420 rpm.

The boil-off rate was 1.9 liters/hr, as measured by the flow meter (see Figure 12) once the background was subtracted. The predicted boil-off results from the hysteretic losses in the superconducting part of the wire and from the eddy currents in the copper cladding. The losses from these two sources for the conditions under which the data were taken amount to 1 liter/hr. The measured and predicted values of the armature losses in the superconducting state are in sufficient agreement to show that the armature should not operate in the superconducting state.

TABLE V. PREDICTED VERSUS EXPERIMENTAL VALUES

Quantity	Predicted	Measured
M	1.17 mh	1.12 mh
$V_a \begin{pmatrix} \omega = 100c/s \\ I_f = 100A \end{pmatrix}$	74 volts (peak)	71 volts (peak)

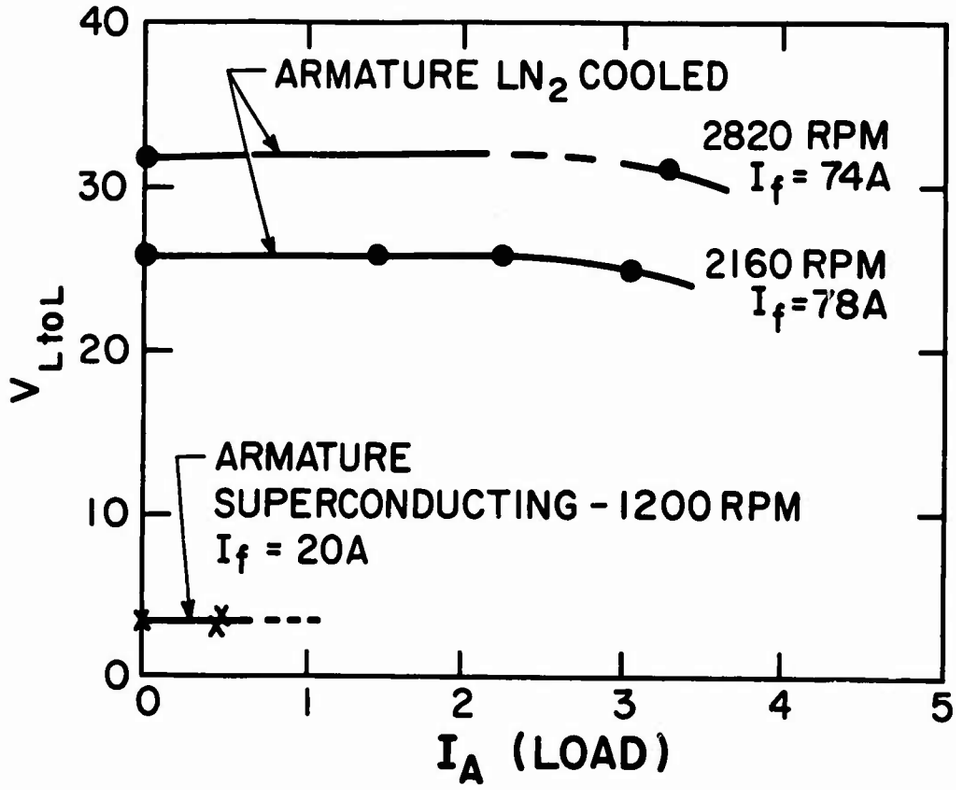

Figure 17. Terminal Characteristics for Unity Power Factor Load.

Figures 9 and 10 show that most of the armature loss at low frequency came from the superconductor, and most of the high frequency loss came from the copper cladding. One can, of course, reduce the copper loss by using unstabilized (or lightly stabilized) superconducting wire for the armature winding. However, for all practical frequencies and at reasonable magnetic field intensity, the armature losses due to the superconductor are still larger than would be acceptable for a machine designed for continuous operation.

3. Motor Tests

A second series of tests was initiated with the aim of operating the superconducting machine as a motor. The experimental equipment was arranged as described in Figure 12, and the test was initiated in the usual way: field superconducting and armature at LN_2 temperature. At liquid nitrogen temperature, the armature was capable of safely carrying a maximum of 10 amperes. It must be remembered that in the nonsuperconducting state only the copper cladding on the superconducting wire is a good electrical conductor.

Figure 13 is a plot of the drag due to windage, brushes, and the drive belt system. Superimposed on these is a plot of the motor input (I_f = 100 A) with the maximum safe current in the nonsuperconducting armature (I_a = 10 A). With the armature at liquid nitrogen temperature, the drive/load DC machine operating as a starting motor could be relieved completely by the superconducting motor. The drag from the belt system and from windage and brush losses is larger than the output of the superconducting machine when the latter's armature is nonsuperconducting. To overcome the losses of the drive system and to obtain useful power from the superconducting motor, the armature must carry more than 30 amperes (i.e., be superconducting).

The mechanical power output of the superconducting motor with its armature at LN_2 temperature was measured by observing the decrease in power consumption of the drive/load DC machine (Figure 12). Figure 13 is a summary of experimental data obtained at low rotational speeds.

The test program was concluded after the data of Figure 13 were obtained.

The data obtained confirmed a few important facts. First, all data agreed well with predictions, using both classical machine theory and the specially derived relationships of Reference 8 for superconducting machinery. Second, the losses of the armature in the superconducting state were of the order of magnitude anticipated and illustrate the necessity of avoiding the exposure of superconducting windings to alternating fields in continuously operating power machinery.

III. MACHINE DESIGN

A. INTRODUCTION

The results obtained in the experimental portion of the program indicated that the relationships derived in Reference 8 can be used with confidence. As a result, these relationships are used in this portion of the report to arrive at a preliminary design for a 3000-horsepower machine suitable for use in helicopters.

The designs that are presented are for air core machines having room-temperature armatures and superconducting field windings. These machines have rotating field windings internal to stationary armature windings. This configuration has been selected for the following reasons:

1. The placement of the rotating member at the smallest possible radius reduces the magnitude of the stresses due to centrifugal forces.

2. The relative ease of transferring power from a stationary armature to and from external circuits.

3. The ease of shielding against a time-varying rather than a stationary field.

B. PRELIMINARY MACHINE DESIGNS

To get an idea of the size and weight of a 3000-horsepower machine, several preliminary designs were carried out. These designs were for machines with air core windings.

Table VI is a summary of the design equations that were utilized. These equations were derived from Reference 8.

Aside from the power, rpm, and electrical frequency of a machine, the armature and field current densities must be known before a suitable design can be generated.

1. Armature Current Density

The maximum overall peak current density J_a in the armature of an experimental 8-kw alternator using superconducting field windings was 770 A/cm^2.[1,2] Conventional machines have current densities of 1500-2000 amperes rms/in.^{2} of conductor, which correspond to peak current values of 330-440 amperes/cm^2.

Since weight is a factor, a value halfway between these has been chosen for the calculations; namely, a peak current density of 600 A/cm^2 in the armature copper. If one assumes a packing factor of $\lambda_a = 0.6$, then the peak overall armature current density J_a is 360 A/cm^2. This is the value used in the calculations.

Table VI shows that power density varies as the overall peak armature current density J_a to the 0.6 power, so that if the current density were lowered to the upper range of conventional machines, the increase in machine volume would be about 23%.

It was felt that the use of the higher current density in the calculations is consistent with the aim of lightweight machines, although heat transfer calculations are necessary to finalize the detailed design of the armature.

2. Current Density in the Superconducting Field Winding

The current-carrying capacity of a superconductor decreases with increasing magnetic field. Figure 18 is a composite plot showing the overall winding current density that has been achieved versus the magnetic field that has been generated in various superconducting coils.

The straight line labeled $J.B = 5.5 \times 10^4$ (A/cm^2) (Wb/m^2) is representative of what can be achieved using current superconducting coil technology, and it is used in determining the field current density in the following way: For each particular geometry of superconducing field winding, there is a point in the field winding where the magnetic field is a maximum. This maximum point determines the current density at which the field will operate, so that the product of the overall field current density $J_f(A/cm^2)$ times the maximum field in the winding $B(Wb/m^2)$ is equal to 5.5×10^4. This product was used in the design presented herein.

3. Machine Geometry

The equations for the mutual inductance between the armature and field M, the armature resistance R_a, and self-inductances of the armature and field L_a and L_f, as well as the power P, are given for a general air core machine, as shown in Figure 19, as a function of the geometry of the machine, its mechanical frequency of rotation ω_m, the overall armature current density J_a, and the field current density J_f.

Also given are simplified formulas for the case where the ratio of outside length to radius of the machine is equal to the value which results in a machine of minimum volume for the particular power level required.

TABLE VI. SUMMARY OF DESIGN EQUATIONS FOR SYNCHRONOUS MACHINES WITH ARMATURE OUTSIDE
(J_f = constant)

Parameter	No. of pole pairs $p \neq 2$	No. of pole pairs $p = 2$
M Mutual Inductance Armature-Field	$\frac{48\,\mu_o N_a N_f \ell_m}{\pi^3 p(4-p^2)} \left(\frac{R_2}{R_o}\right)^p \frac{(1-x^{-p+2})(1-y^{p+2})}{(1-x^2)(1-y^2)}$	$\frac{6\,\mu_o N_a N_f \ell_m (1+y^2)}{\pi^3 (1-x^2)} \left(\frac{R_2}{R_o}\right)^2 \ln\frac{1}{x}$
R_a Armature Resistance per phase	$\frac{21\,\rho_a N_a^2}{2\,p\,\lambda_a R_o (1-x)}$	same as for $p \neq 2$
L_a Armature Self Inductance	$\frac{36\,\mu_o N_a^2 \ell_m \left[(p-2)-(p+2)x^4+4x^{p+2}\right]}{\pi^3 p(p^2-4)(1-x^2)^2}$	$\frac{18\,\mu_o N_a^2 \ell_m \left[\frac{1}{4}(1-x^4)+x^4 \ln x\right]}{\pi^3 (1-x^2)^2}$
L_f Field Self- Inductance	$\frac{16\,\mu_o N_f^2 \ell_m \left[(p-2)-(p+2)y^4+4y^{p+2}\right]}{\pi^3 p(p^2-4)(1-y^2)^2}$	$\frac{8\,\mu_o N_f^2 \ell_m \left[\frac{1}{4}(1-y^4)+y^4 \ln y\right]}{\pi^3 (1-y^2)^2}$
P Power	$\frac{6}{\pi}(\mu_o \omega_m J_a J_f R_o^5 \cos\theta)\left[\frac{\ell_T}{R_o}-\frac{\pi}{4p}(1+x)\right]\frac{(x-\delta)^{p+2}(1-x^{-p+2})(1-y^{p+2})\cos\theta}{p(4-p^2)}$	$\frac{3}{4\pi}(\mu_o \omega_m J_a J_f R_o^5 \cos\theta)\left[\frac{\ell_T}{R_o}-\frac{\pi}{8}(1+x)\right](x-\delta)^4(\ln\frac{1}{x})(1-y^4)$

$(\ell_T/R_o)_{opt.}$ Overall Length to Radius Ratio	$\frac{2.5\pi}{4p}(1+x)$	same as for $p \neq 2$
R_o Outside Radius $(\ell_T/R_o)_{opt.}$	$\left[\frac{4p(4-p^2)P}{9\mu_o\omega_m J_a J_f (x-\delta)^{p+2}(1-x^{-p+2})(1-y^{p+2})(1+x)\cos\theta}\right]^{0.2}$	$\left[\frac{32P}{9\mu_o\omega_m J_a J_f (x-\delta)^4 \ln\frac{1}{x}(1-y^4)(1+x)\cos\theta}\right]^{0.2}$
$\left[\frac{P}{V}\right]\left(\frac{\ell}{R_o}\right)_{opt.}$ Power Density	$\frac{9}{2.5\pi^2}\left(\frac{4}{9}\right)^{0.4}\left(\mu_o\omega_m J_a J_f\cos\theta\right)^{0.6} P^{0.4}\left[\frac{p^{2/3}(x-\delta)^{p+2}(1-x^{-p+2})(1-y^{p+2})}{(4-p^2)(1+x)^{2/3}}\right]^{0.6}$	$\frac{9}{2.5\pi^2}\left(\frac{4}{9}\right)^{0.4}(\mu_o\omega_m J_a J_f\cos\theta)^{0.6} P^{0.4}\left[\frac{2^{2/3}(x-\delta)^4(1-y^4)\ln\frac{1}{x}}{4(1+x)^{2/3}}\right]^{0.6}$
$x_a = \frac{\omega L_a I_a}{V_a}$ Normalized Synchronous Reactance $(\ell_T/R_o)_{opt.}$	$-\frac{J_a\left[(p-2)-(p+2)x^4+4x^{p+2}\right]}{4J_f(x-\delta)^{p+2}(1-x^{-p+2})(1-y^{p+2})}$	$\frac{J_a\left[\frac{1}{4}(1-x^4)-x^4\ln x\right]}{J_f(1-y^4)(x-\delta)^4\ln\frac{1}{x}}$
$\frac{I_a R_a}{V_a}$ Normalized Armature Joule Loss ℓ_T/R_o opt.	$\frac{7\pi^2}{36}\left(\frac{\rho_a}{\mu_o\lambda_a\omega_m R_o^2}\cdot\frac{J_a}{J_f}\right)\frac{(4-p^2)(1-x^2)}{(x-\delta)^{p+2}(1-x^{-p+2})(1-y^{p+2})}$	$\frac{7\pi^2}{9}\left(\frac{\rho_a}{\mu_o\lambda_a\omega_m R_o^2}\cdot\frac{J_a}{J_f}\right)\frac{(1-x^2)}{(1-y^4)(x-\delta)^4\ln\frac{1}{x}}$
$\frac{V_a}{S_a}$ Volts per Turn of Armature $(\ell_T/R_o)_{opt.}$	$\frac{9}{\pi}(\mu_o\omega_m R_o^3 J_f)\frac{(x-\delta)^{p+2}(1-x^{-p+2})(1-y^{p+2})}{p(4-p^2)(1-x)}$	$\frac{9}{8\pi}(\mu_o\omega_m R_o^3 J_f)\frac{(x-\delta)^4(\ln\frac{1}{x})(1-y^4)}{(1-x)}$
$\frac{\omega_m E_f}{[P]_{pF}}$ Magnetic Field Energy $(\ell_T/R_o)_{opt}$	$-\frac{2}{3}\frac{J_f}{J_a}\frac{(x-\delta)^{3-p}(1+y)\left[(p-2)-(p+2)y^4+4y^{p+2}\right]}{p(1+x)(1-x^{-p+2})(1-y^{p+2})}$	$\frac{J_f}{6J_a}\frac{(x-\delta)(1+y)\left[(1-y^4)+4y^4\ln y\right]}{(1+x)(\ln\frac{1}{x})(1-y^4)}$
$(B_f)_{max}$ Maximum Magnetic Field in Winding	$\frac{2}{\pi}\mu_o J_f R_o (x-\delta) f(y,p)$	same as for $p \neq 2$

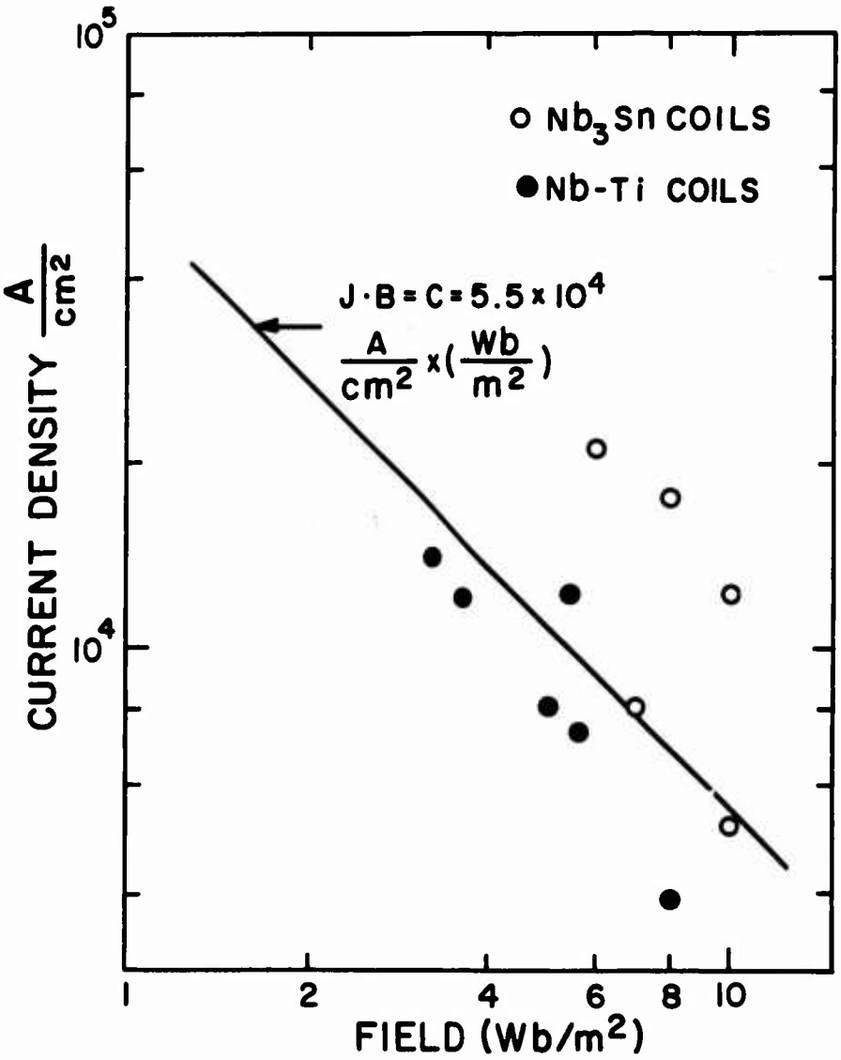

Figure 18. Current Density Versus Magnetic Field for Superconducting Coils Presently in Use. Shown Also Is the Curve Selected for the Machine Designs Presented in This Report.

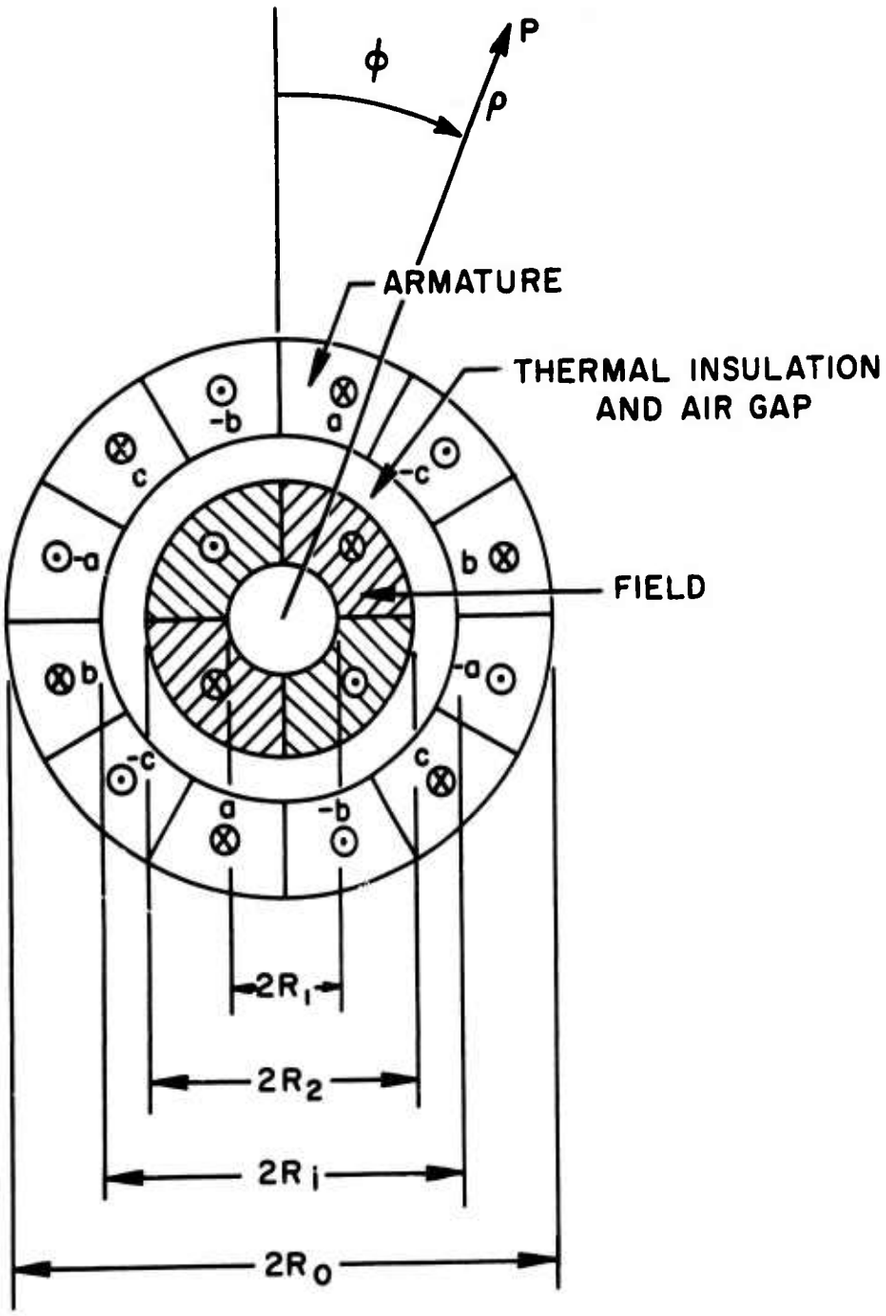

Figure 19. Geometry of General Air Core Machine.

It was shown in Reference 8 that the machine weight was not too sensitive to variations in the armature radius ratio $x = R_i/R_o$ and the field radius ratio $y = R_1/R_2$. Therefore, for these preliminary designs, values of $x = 0.75$ and $y = 0.3$ were chosen for all designs. (These are very close to the optimum values.)

Using these values, together with those of Table VII, the designs presented in Table VIII were generated. The power level is 2.2 mw at unity power factor. The electrical frequency in all cases was 400 cycles, so that as the number of pole pairs increased, the rpm decreased.

C. CRYOGENIC DESIGN

1. Liquid Helium Coolant

The superconductor requires temperatures at least as low as $18^{\circ}K$ (Figure 20). Liquid helium is best suited for producing the low temperatures needed to maintain superconductivity. The phase diagram of He^4 is shown in Figure 21. The normal boiling point is $4.2^{\circ}K$, and the critical temperature is $5.1^{\circ}K$ (2.3 atm). Liquid helium exists in two phases, He I and He II, separated by a phase boundary commonly called the λ - line. At saturated vapor pressure, this transition occurs at the temperature $T_\lambda = 2.19^{\circ}K$, which is termed the λ - point. Although He I behaves as an ordinary fluid, He II, owing to quantum effects, does not. The outstanding features of He II are its extremely high thermal conductivity ($\approx 10^3$ times that of room-temperature copper) and its abnormally low viscosity.

Therefore, there are three helium fluids with which to cool the superconductor: sub-λ helium (He II), normal helium (He I) at its boiling point, and supercritical helium (He I).

For the present application, only machines having superconducting field windings will be considered. The armature will be operated at room temperature; as a consequence, the cryogenic problem is confined to that of providing a liquid helium environment for the field windings only.

For proper operation, there must be a continuous flow of coolant (liquid helium) to the superconducting winding under all operating conditions of the generator. Since cooling of the field must be accomplished when the generator is stopped or rotating and under all flight conditions of the helicopter, gravity cannot be used to carry the coolant liquid to the various parts of the field. The helium must be fed under pressure to the superconducting field windings. As shown in Figure 21, the physical characteristics of liquid helium change with pressure. The heat transfer from the

TABLE VII. SUMMARY OF MACHINE PARAMETERS
$x = 0.75$
$y = 0.3$
power = 2.2 mw at unity p.f.
$\omega = 400$ c/s
$\lambda_a = 0.6$
$J_a = 360 \times 10^4$ A/m^2
$\rho_a = 2 \times 10^{-8}$ Ω - m
$\Delta = 0.0254$ m

TABLE VIII. SYNCHRONOUS MOTOR SIZES
(400 c/s)

Power (mw)	P Pole Pairs	Speed (rpm)	R_i (m)	R_2 (m)	R_2' (m)	R_0 (m)	wt (lbs)
2.2	1	24,000	.018	.060	.085	.114	326
2.2	2	12,000	.036	.012	.145	.194	415
2.2	3	8,000	.054	.180	.205	.274	524
2.2	4	6,000	.072	.240	.265	.354	650

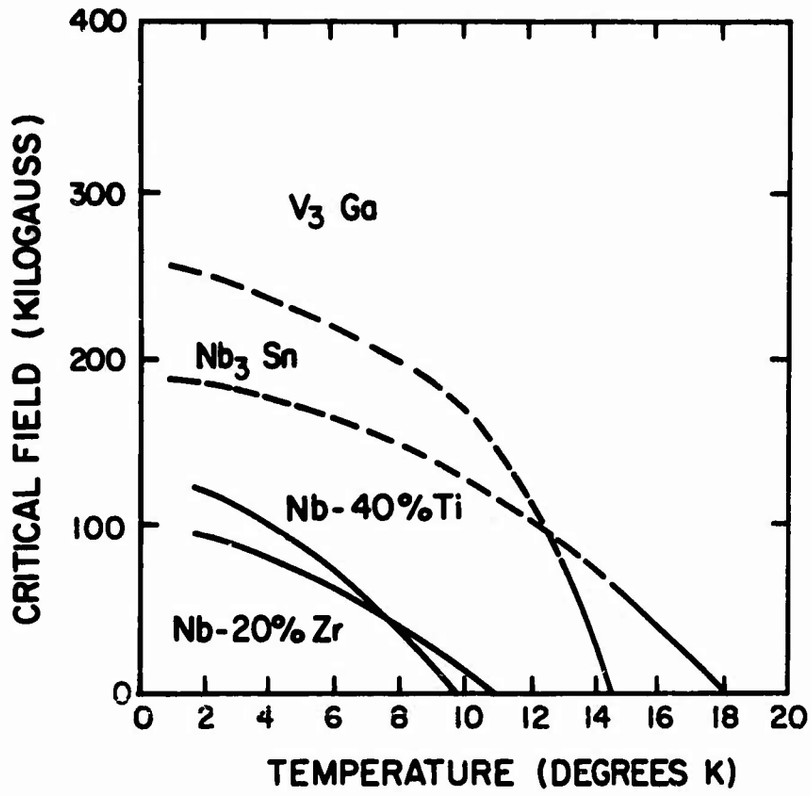

Figure 20. Critical Fields for Various Superconductors.

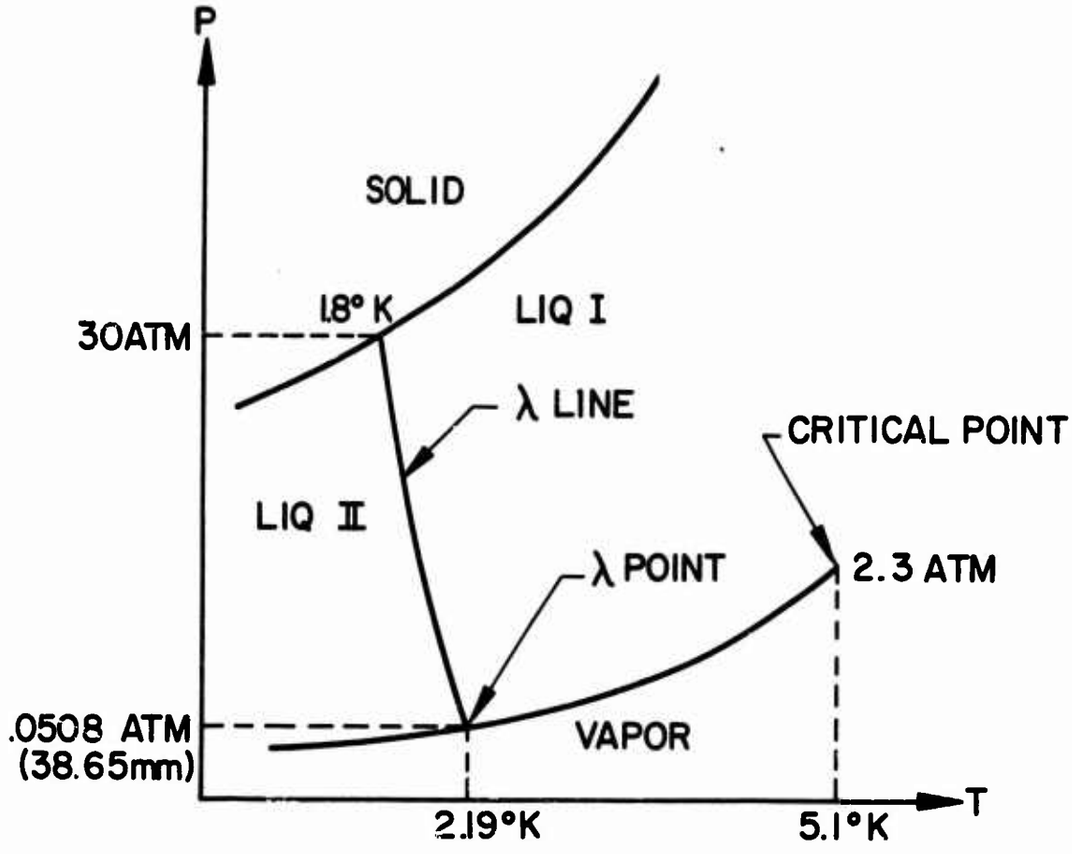

Figure 21. Phase Diagram for Helium.

superconductor to the liquid bath is also pressure dependent. The pressure under which liquid helium is to be fed to the field winding must therefore be chosen carefully to ensure conditions of good heat transfer between superconductor and liquid.

One technique developed by Avco to determine the stability of superconducting windings is to insert a heater into a superconducting coil. The coil is immersed in liquid helium, and it is charged to a current that is in the vicinity of its quench current. A pair of voltage taps is attached across the coil terminals, and the current to the heater is slowly increased. As long as the voltage taps read zero volts, the coil is superconducting (Figure 22). As the heater current is increased, a slight controlled rise in voltage will indicate that the current is shared[11] between the superconductor and the copper substrate. A sharp rise in voltage (Figure 22) indicates that a normal region is formed and therefore the coil is no longer all superconducting. The heater current is then decreased until the coil recovers (Figure 22) to an all superconducting state. Ideally, for good operation, the recovery point should be as close as possible to the takeoff point. During a series of experiments at Avco Everett Research Laboratory, it was found that the takeoff and recovery points of coils are strong functions of the ambient pressure on the liquid helium. Figure 23 gives the results of tests performed at Avco, showing the recovery and takeoff points of a coil as functions of helium pressure. It is quite clear from these results that the liquid helium must be pressurized above its critical point for proper operation. In the present application, we will therefore use supercritical helium at about 20 psig.

The use of a pressurized cooling fluid requires that the cooling loop be completely closed. This will necessitate a rotary joint in the liquid helium transfer line. Although rotary seals suitable for operation at liquid helium exist,[12] no rotary joint for liquid helium transfer lines is commercially available at present. However, using the available off-the-shelf industrial seals, it is possible to design such a joint (Figure 24). It is estimated that the seal lifetime will be of the order of a few thousand hours (wear rate is approximately 0.00001 in./hr). This lifetime can be arbitrarily increased by increasing the thickness of the carbon insert (Figure 24). We can therefore make the seal lifetime equal to the number of hours between overhauls of the prime mover. The heat leak from this joint to the liquid helium is estimated to be about 50×10^{-3} watts. Assuming that no use is made of the sensible heat of the helium gas between 4°K and 77°K, this heat leak will result in a liquid helium consumption of 70 cc/hour. Therefore, the problem of feeding liquid helium under pressure to a rotating field winding appears to be quite soluble.

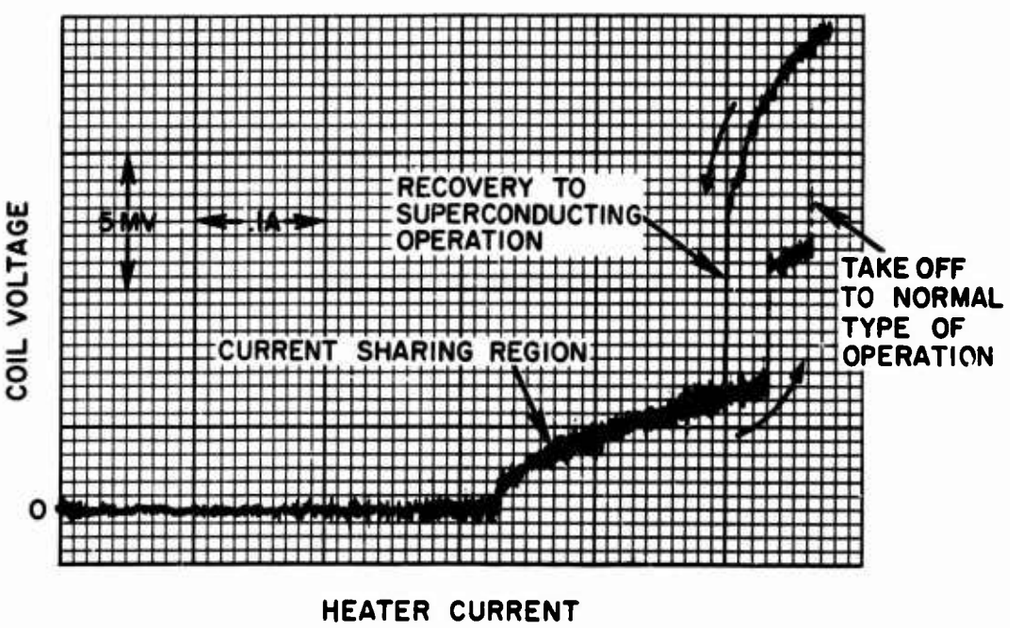

Figure 22. A Heater Plot Showing Typical Two-Dimensional Behavior at a Magnet Current of 550 Amperes.

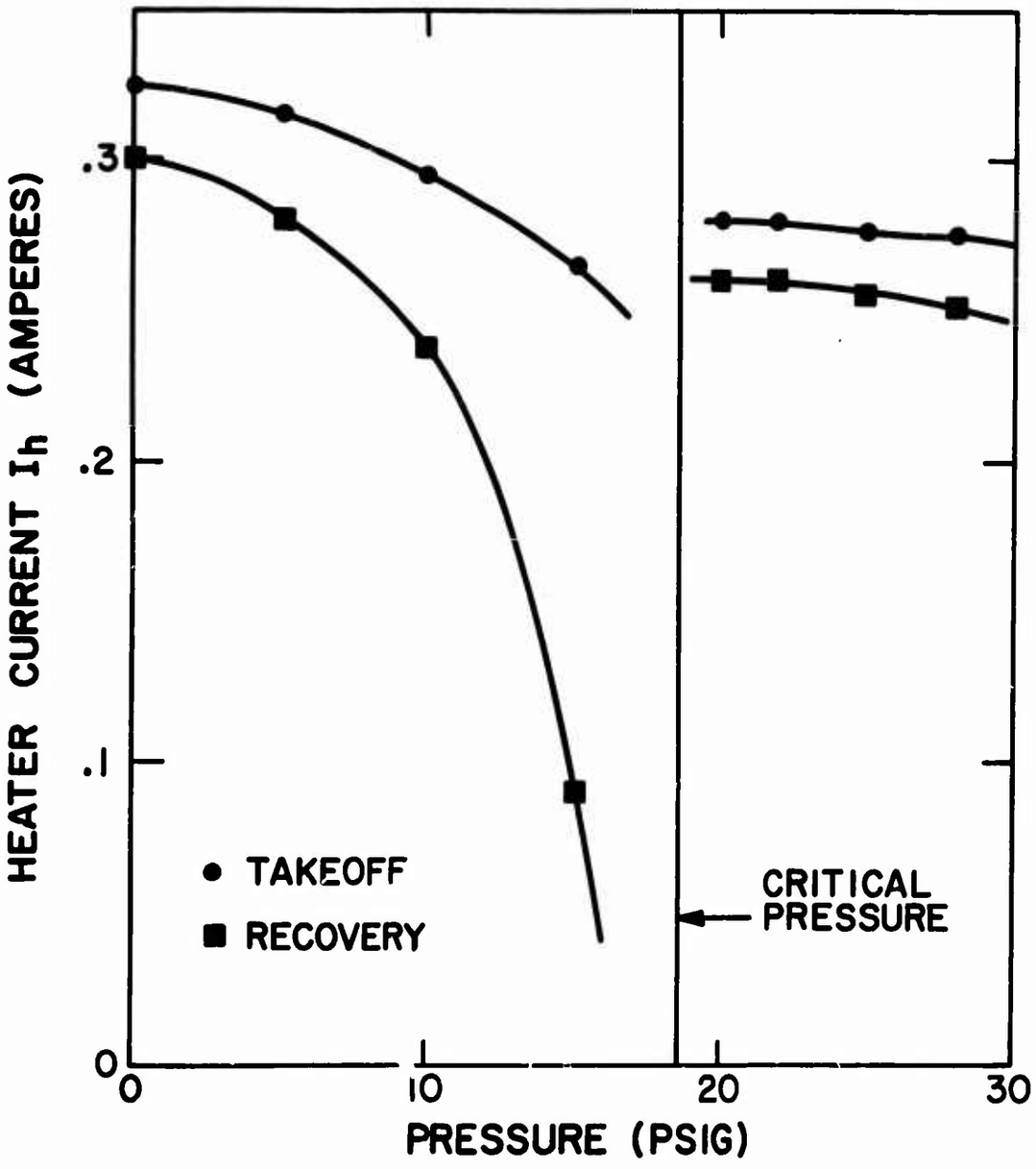

Figure 23. Heater Current at Takeoff and Recovery Versus Helium Pressure at a Magnet Current of 620 Amperes.

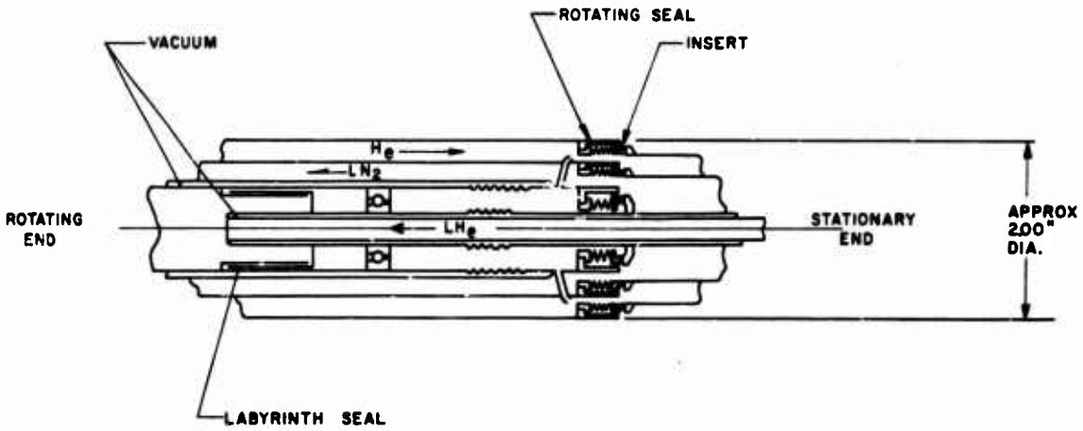

Figure 24. Rotary Joint in Liquid Cryogen Transfer Line.

2. Dewar Construction

For the purpose of calculating typical heat leaks and material stresses of the Dewar, it is assumed that the field has an OD of 0.2 meter and a length of 0.6 meter. These are median values for the machines considered in Section II. A. 1. Drawing on past experience in the building and testing of superconducting alternators, the following Dewar design is presented (Figure 25). Figure 25 is an open-ended Dewar that uses LN_2 stations and the helium return vapors to cool the warm ends of the Dewar. This reduces the heat leaks to an absolute minimum.

An estimate of the heat leak associated with the open-ended Dewar (Figure 25) follows. As will be seen in the next section, a Dewar wall thickness of 0.050 inch possesses sufficient strength to withstand the operational torque of the machine. For a properly designed and built Dewar, the main heat leak to the liquid helium region is from heat conduction down the Dewar walls. Under ordinary laboratory operation, it is possible to absorb the majority of this heat leak by channeling the helium boil-off vapors along the inner Dewar walls. However, in our operation, the boil-off vapors must be split between both ends of the Dewar and must cool both the Dewar walls and the field energizing leads, if such leads are used. The possibility of doing away with the high ($\approx$300 amps) field energizing leads in favor of a flux pump will be explored later. The amount of cooling available from the helium boil-off gas is therefore uncertain because of the many parallel escape paths available to the gas. For the sake of this discussion, the cooling available from this gas will be ignored. This will give a conservative value for the heat leak.

The heat leak path occurs through the two stainless steel sleeves that form the end of the Dewar. Their dimensions and properties are:

Length = 10 cm

Circumference = 63.6 cm

Thickness = 0.127 cm

$k_{s.s} \doteq 30 \times 10^{-3}$ watts/cm^{o}K

$\Delta T = 80^{o}$K

The heat leak associated with the two sleeves is

$$Q = \frac{2 \times 30 \times w^{-3} \times 63.6 \times 0.127 \times 80}{10}$$

$$= 3.85 \text{ watts}$$

To this must be added the heat leak from the field energizing leads. A well-designed vapor-cooled lead will require 1.5 liters/hour of liquid helium for each 1000 amperes[13] of current. At the field energy

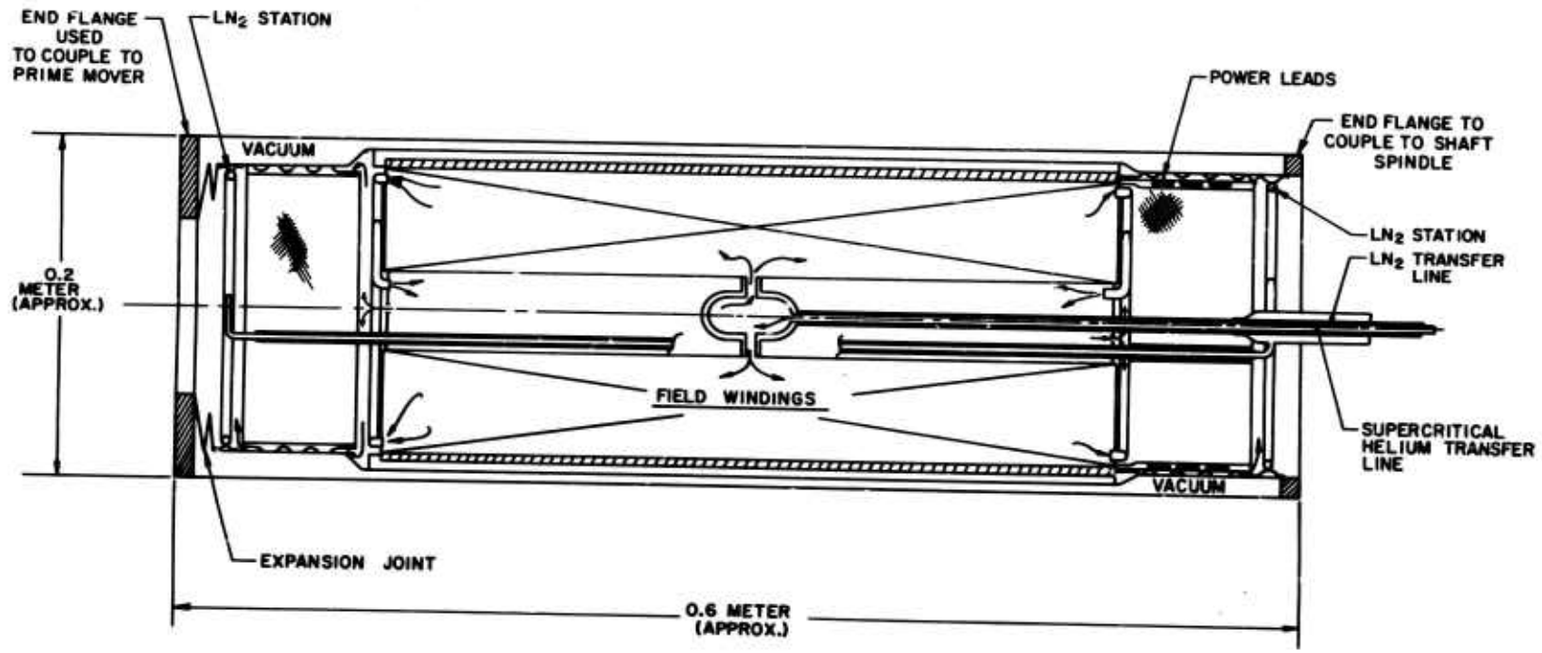

Figure 25. Double-Ended Dewar Design for Superconducting Motor.

levels required for the machines outlined in Section II. A. 1, the field energizing leads carry between 300 and 400 amperes and provide reasonable field charge times. These leads will cause an additional liquid helium boil-off of about 0.5 liter/hr.

Therefore, the total liquid helium refrigeration requirement may be fixed at 4.5 watts. As stated originally, the heat leak from both Dewar designs will be quite similar. Since no use is made of the helium boil-off vapors, this value of heat leak is on the conservative side.

3. Refrigerators

Figure 26 (obtained from Reference 14) shows refrigerator weight versus refrigerator capacity at 4.2°K. The curve labelled reciprocating machinery refers to machines commonly used in the laboratory, where weight reduction is given very little consideration. The curve labelled turbomachinery refers to the anticipated performance of helium liquefiers presently in the experimental stages. These machines are expected to be available within a few years. Presently, lightweight refrigerators weighing about 100 lbs/watt are available commercially. The weight of the 5-watt refrigerator will range between 500 and approximately 150 pounds (depending on how soon the refrigerator is required).

D. MECHANICAL DESIGN

The main consideration in the mechanical design of the superconducting alternator is to fabricate a structure that causes the minimum heat leak to the liquid helium region while possessing enough strength to withstand the operational loads. The very large field energies available in superconducting machines require a considerable amount of banding around the field winding. If the air gap is to be a minimum, this banding material must have a high tensile strength.

The torque from the shaft is transmitted to the field through the inner Dewar wall. This wall must therefore take the full operational load of the machine. The shear stress in the thin inner walls of the Dewar is given by (for a wall thickness of 0.050 inch)

$$\tau = \frac{M_t}{2\pi R^2 t} = \frac{\text{Applied torque}}{2\pi\,(\text{mean radius})^2\,(\text{thickness})}$$

A 2.2 mw, 6000-rpm machine is subjected to 2580 ft-lbs of torque under steady-state operation. This causes a shear stress of

$$\tau = \frac{2580 \times 12}{2\pi\,(16) \times .050}$$

$$= 6150 \text{ psi}$$

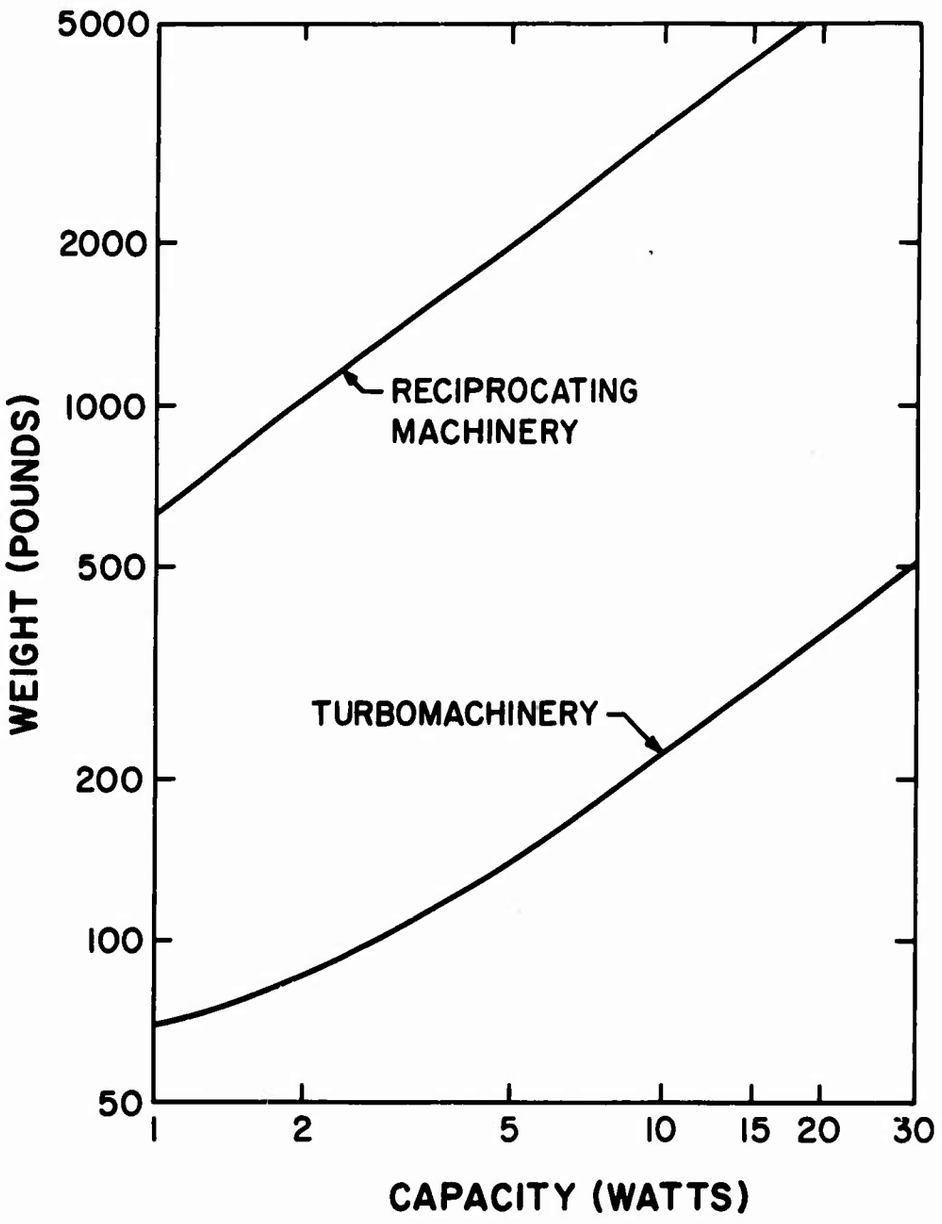

Figure 26. Refrigerator Weight Versus Refrigerator Capacity at 4.2°K.

This is a most conservative stress level for stainless steel. The thickness of the inner Dewar wall could easily be reduced to achieve a smaller heat leak. However, a thinner Dewar wall might cause field alignment problems during construction. It has been our experience, with this type of construction, that thin walls tend to warp while being welded, thereby throwing the field winding out of center with the end flanges of the Dewar. A 0.050-inch-thick wall will be used for this example.

There are many other interrelated problems associated with the mechanical design of a superconducting motor. These include the critical frequency of the rotor, bearing life time, armature cooling requirements, and shock resistance of various parts. Additionally, when a motor is considered for use on board a helicopter, the mechanical design must take into account the additional requirements imposed on it because of its environment.

A possible motor configuration is drawn in Figure 27. This motor is shown in the horizontal position, but it is, in fact, independent of orientation for proper operation.

E. CONFORMANCE TO MILITARY SPECIFICATIONS

From experience that AERL has accumulated through study programs and experimental work with superconducting machinery, it can be anticipated that the incorporation of superconducting machinery into the existing system can be accomplished with minimal interface problems. The Military Specification covering power equipment contains no requirements that appear to be too difficult to meet with superconducting machinery. However, the special nature of superconductors and their cryogenic equipment will require additional consideration and construction techniques that, although not incompatible with present methods, will best be met by new methods and unconventional technology. Some aspects of these new devices and technology will be explored below, along with a few main requirements that apply to rotating machinery in general.

1. Oil Seals

Accepted procedure is to use nonrubbing oil seals on the shaft. This can be done for the bearing oil seals on superconducting machines. However, the necessity of feeding pressurized liquid helium to a rotating field winding requires the use of friction-type seals on the transfer line (Figure 24). The types of seals depicted in Figure 24 have performed satisfactorily in environments as diversified as jet engines and on the cryogenic side of rocket engines. The only apparent drawback of this type of seal is that one of the rubbing surfaces (carbon insert in the present case) wears out. Since, as stated in the previous section, the wear rate is extremely small, the lifetime of the seal can be adjusted to match the lifetime of any other piece of equipment desired, by the simple expedient of using a thicker insert. At the reported wear rate of 1×10^{-5} inches per hour for a 2-inch-diameter seal rotating at 4000 rpm, a thickness of 0.10 inch would give a 10,000-

hour lifetime. Relatively small seal thicknesses give very large lifetimes, and the finite lifetime of these seals should not present undue maintenance problems.

2. Vibration

Balancing the rotor of a superconducting rotating machine presents special problems because of the particular construction of the rotor. The rotor is a double-walled cylinder (Dewar) with most of the weight supported by the inner wall. Since the outer wall of the Dewar is relatively light compared to the field winding, it is assumed that the totality of the out-of-balance weight of the rotor will be due to the field winding. However, in the process of balancing the rotor, it is impossible to add weights to the field since it is enclosed within the Dewar walls. Weights added to the outside wall will cause the rotor to run smoothly, but they will not prevent the inner wall of the Dewar from deforming under the influence of the field out-of-balance weight. The initial balancing must therefore be done at low speed, with weights added to the outside wall until the rotor runs smoothly. The rotor is then stopped, the field is withdrawn from the Dewar, and the weights are added directly to the field. The field is reinserted into the Dewar and final balancing is done. This procedure was followed with the experimental machine with excellent results. Balancing to 5500 rpm was achieved in one balance operation. The weights were then transferred to the field winding, and the rotor stayed within the balance region with the out-of-balance vibrations below the measuring instrument's perception level.

3. Field Construction

Generally, Military Specifications require that field coils (pole windings) be interchangeable between machines of the same type.

It is difficult to build superconducting field windings individually, by pole. However, so far it has been the practice of winding the field in such a way that all poles of the field form a single unit. This makes the interconnection between poles easier and much more secure. It also permits the whole field structure to be inserted into a "can" that serves both as the banding structure and as the liquid helium container, making a strong and compact unit. Figure 3 shows the two-pole superconducting field winding for the experimental machine. Clearly visible is the sandwich-type construction of this winding. Ten oval pancakes of Nb_3Sn are sandwiched between the two stainless steel pole pieces. Also visible are the vertical cooling passages that distribute the liquid helium to all the faces of the pancakes. This field winding was then inserted into a 3/8-inch-thick stainless steel can (Figure 4) that is used both as the banding structure and as the liquid helium container. Figure 4 shows the outside of this can, the insulating plug, and the spiral vapor-cooled leads attached to the field. As can be seen, this type of construction gives the maximum number of

conductors per unit volume. If the poles of the field were each wound separately and individually attached to a common anchor point for individual removal, valuable space would be lost and the power density of the machine would suffer. However, if the power density of the machine is relatively unimportant, the latter type of construction is easily practicable.

If the construction method exhibited in Figures 3 and 4 is used, individual poles of a field winding cannot be easily replaced. Under actual operation, the easiest way to replace a defective pole would be to remove the whole field winding as depicted in Figure 4 and drop a prebalanced spare winding into the Dewar.

4. Field Excitation

The output voltage of the field exciter is determined by the limits imposed on the charge-up time of the field winding. Superconducting windings suffer AC losses during charge-up to their full current-carrying capacity. If these losses can be absorbed by the system's supply of cryogens, then the charge-up time is limited only by the ouput voltage of the exciter. Once charged, the only voltage drop in the field excitation circuit will occur across the copper room-temperature leads and across the brushes. As such, during steady-state operation, a 2-to-3-volt power supply giving the required amperage is sufficient. Such an exciter could easily be run off the prime mover.

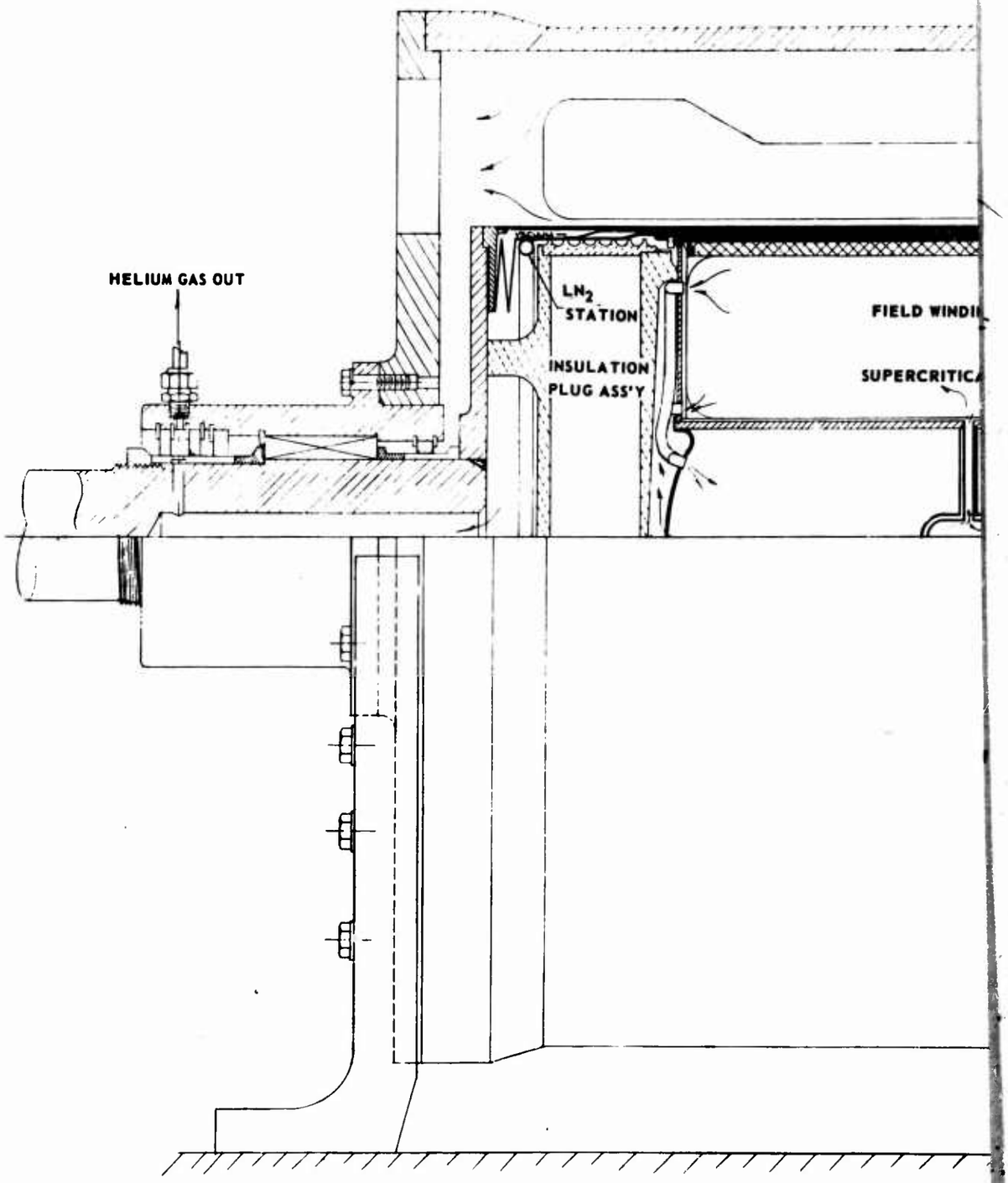

Figure 27. Assembly Layout of Typical Motor With Superconducting Field.

A

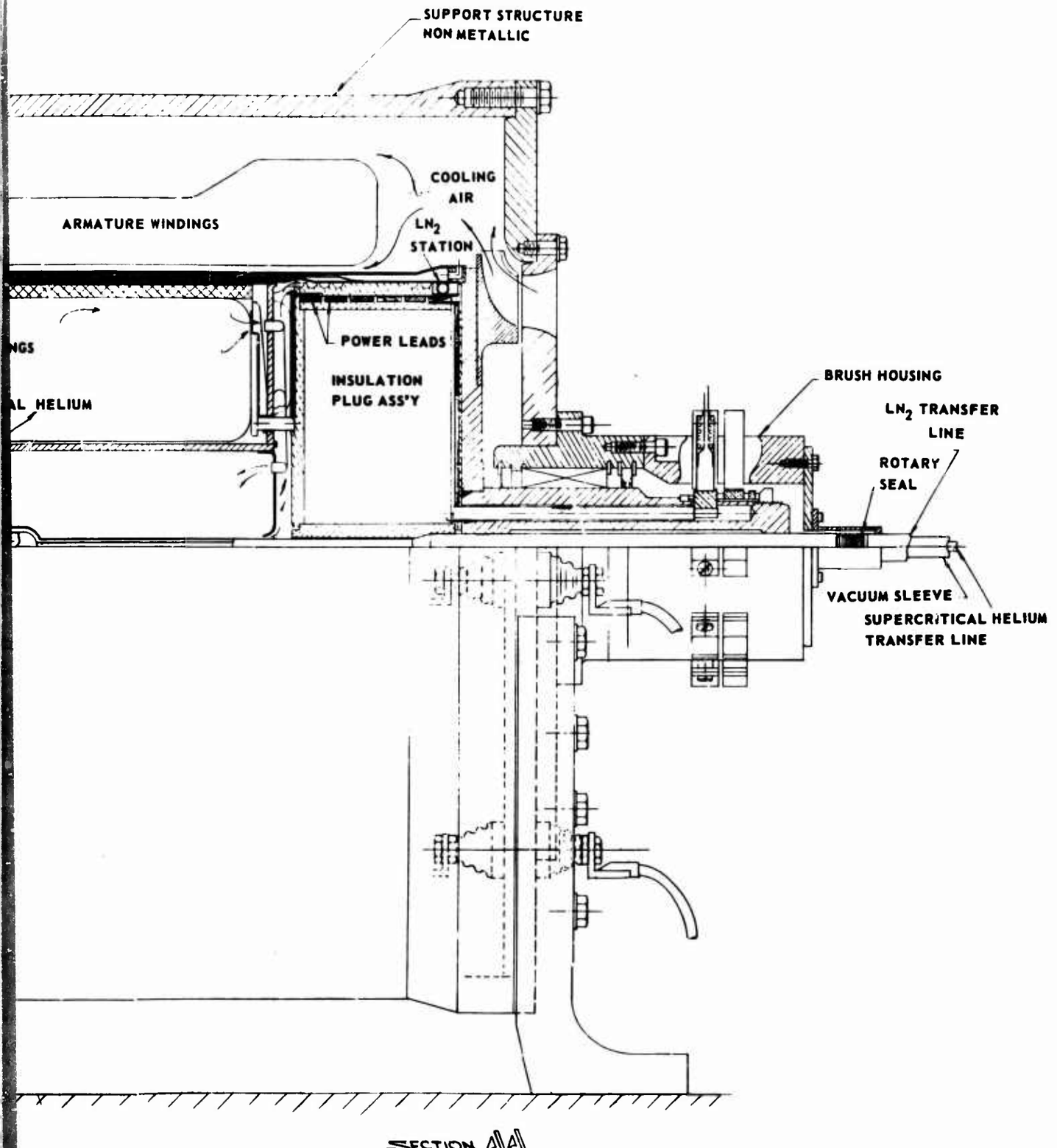
SUPPORT STRUCTURE
NON METALLIC
COOLING
AIR
ARMATURE WINDINGS
LN_2
STATION
POWER LEADS
INSULATION
PLUG ASS'Y
BRUSH HOUSING
LN_2 TRANSFER
LINE
ROTARY
SEAL
VACUUM SLEEVE
SUPERCRITICAL HELIUM
TRANSFER LINE

SECTION AA

B

LITERATURE CITED

1. Woodson, H. H., Stekly, Z. J. J., and Halas, E., A STUDY OF ALTERNATORS WITH SUPERCONDUCTING FIELD WINDINGS: PART I - ANALYSIS, IEEE, Transaction of Power Apparatus and Systems, Vol. PAS-85, No. 3, March 1966.

2. Stekly, Z. J. J., et al., A STUDY OF ALTERNATORS WITH SUPERCONDUCTING FIELD WINDINGS: PART II - EXPERIMENT, IEEE Transaction on Power Apparatus and Systems, Vol. PAS-85, No. 3, March 1966.

3. McFee, R., APPLICATION OF SUPERCONDUCTIVITY TO THE GENERATION AND DISTRIBUTION OF ELECTRIC POWER, Electrical Engineering, February 1962.

4. Klaudy, P. A., SOME EXPERIMENTS RELATING TO THE LAYOUT OF SUPERCONDUCTING TRANSFORMERS, Advances in Cryogenic Engineering, Vol. 9, 1964.

5. DiSalvo, F., AC LOSSES IN TYPE II SUPERCONDUCTORS, AMP 206, Avco Everett Research Laboratory, Everett, Massachusetts, 1966.

6. Mark's MECHANICAL ENGINEERS' HANDBOOK, Sixth Edition, New York, McGraw-Hill Book Company, 1958.

7. Fitzgerald, A. E., Kingsley, C., Jr., ELECTRIC MACHINERY, Second Edition, New York, McGraw-Hill Book Company, 1961.

8. Stekly, Z. J. J., et al., STUDY OF POTENTIAL SIZE AND WEIGHT REDUCTIONS IN MARINE ELECTRIC PROPULSION MACHINE BY UTILIZING SUPERCONDUCTORS, Final Report, Contract No. Nobs-94528, Avco Everett Research Laboratory, Everett, Massachusetts, 1968.

9. Bean, C. P., et al., A RESEARCH INVESTIGATION OF THE FACTORS THAT AFFECT THE SUPERCONDUCTING PROPERTIES OF MATERIALS, Technical Report No. AFML-TR-65-431, General Electric Company, Schenectady, New York, March 1966.

10. Gourishankar, V., ELECTROMECHANICAL ENERGY CONVERSION Scranton, Pennsylvania, International Textbook Company, 1965.

11. Stekly, Z. J. J., and Zar, J. L., STABLE SUPERCONDUCTING COILS, Avco Everett Research Laboratory Research Report 210, Everett, Massachusetts, March 1965.

12. SEALS, Reference Issue, Machine Design, Vol. 39, March 1967.

13. Stekly, Z. J. J., Zar, J. L., and Hoppie, L., DESIGN OF SUPER-CONDUCTING MAGNET SYSTEMS, Technical Report AFAPL-TR-66-126, Vol. 1, Air Force Propulsion Laboratory, Wright-Patterson Air Force Base, Ohio, February 1967.

14. Gessner, R. L., and Colyer, D. B., MINIATURE CLAUDE AND REVERSE BRAYTON CYCLE TURBOMACHINERY REFRIGERATORS, Paper No. F-5, Presented at the Cryogenic Engineering Conference, Stanford University, Stanford, California, August 21-23, 1967.

15. Greeneisen, D. P., A DESIGN PROGRAM FOR SUPERCONDUCTING ELECTRICAL MACHINES, Master's Degree Thesis at M.I.T., May 1968.

APPENDIX

CALCULATION OF THE NO-LOAD COPPER LOSSES

A. MODEL

As already described, the armature conductors for the test machine were a composite of superconducting material (niobium-titanium) and copper cladding. The outside diameter of the superconducting material is 11 mils, while the outside diameter of the copper cladding is 20 mils. The inner and outer edges of the armature conductor are exposed to different intensities of flux. Consequently, a voltage difference will exist, in which case eddy current losses are expected. The purpose of this appendix is to estimate these armature losses. It is important to note that these losses will exist without armature current.

An exact expression for these losses would be very difficult to obtain, even if an acceptable model could be agreed to beforehand. The analysis given here is a worst-case analysis, in that in the actual case the superconductor will in all probability redistribute the flux so that the difference assumed in this analysis will not exist, and the losses will be lower than those predicted by the present analysis.

To make the mathematics tractable, the circular conductor is assumed to be made up of a rectangular superconductor and two rectangular copper areas, as shown in Figure 28. Further, it is assumed that the circulating current is proportional to the voltage difference existing between the voltage induced in the superconductor (assumed to be constant over the superconductor cross section and taken equal to the value calculated at the center y_o) and the filament under consideration. This current is inversely proportional to the resistance of a filament; the return path for the current is assumed to be through the superconductor.

B. ANALYSIS--ACTIVE ARMATURE CONDUCTOR

The flux density[15] is given by the expression

$$B_\rho = \frac{4\mu_o}{3\pi^2} N_f I_f R_2 \left(\frac{1+y+y^2}{1+y}\right)\left[\frac{1}{\rho^2} + \frac{1}{R_s^2}\right] \cos\phi \qquad (1)$$

where

I_f = the field current

μ_o = permeability of free space ($4\pi \times 10^{-7}$)

R_1 = inside radius of the field winding

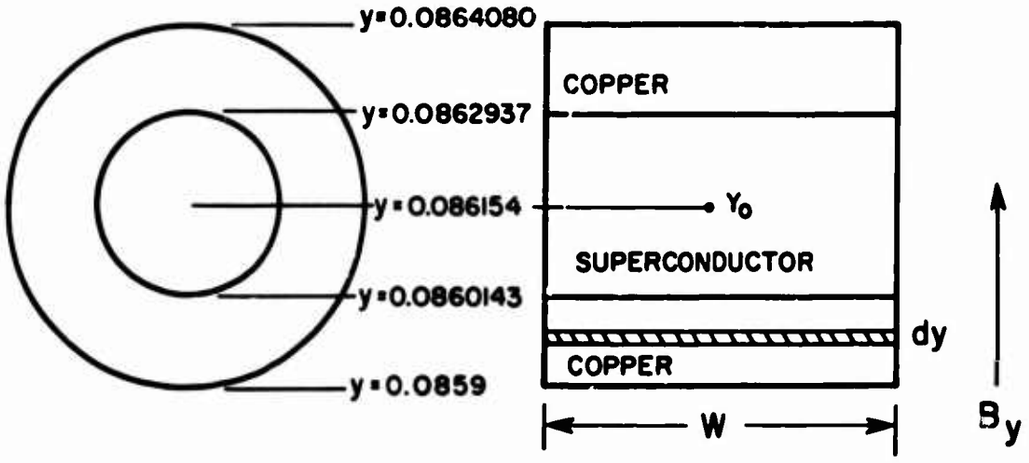

Figure 28. Actual and Assumed Superconductor Cross Sections.

R_2 = outside radius of the field winding

R_s = inside radius of the iron shield

ϕ = angle measured from the axis of the field winding

y = ratio of R_1 to R_2

N_f = number of turns in the field winding

For the test machine, the dimensions and values of various constants are

R_1 = 0.01 meter

R_2 = 0.0571 meter

y = 0.1775

R_s = 0.140 meter

N_f = 3368 turns

Substituting these values yields the following expression for the maximum value of flux at a distance y from the center of the machine:

$$B_y = 3.26 \times 10^{-5} \left[51 + \frac{1}{y^2}\right] I_f \qquad (2)$$

The voltage induced in a filament located at y is

$$e_y = \frac{B_y \ell v}{\sqrt{2}} = \frac{2\pi B_y}{\sqrt{2}} \ell y f \qquad (3)$$

where

ℓ = the length of the conductor

f = the frequency

The voltage at the center (assumed to be constant throughout the superconductor) is

$$e_{y_o} = \frac{2\pi B_{y_o}}{\sqrt{2}} \ell y_o f \qquad (4)$$

The voltage difference which causes the circulating current is

$$\Delta e = e_{y_o} - e_y = \frac{2\pi \ell f}{\sqrt{2}} (B_{y_o} y_o - B_y y) \qquad (5)$$

The resistance in the circulating path is

$$R = \frac{\rho \ell}{w dy} \tag{6}$$

For this case, then, the incremental power loss is

$$dP = \frac{\overline{\Delta e}^2}{R} = \frac{2\pi^2 \ell f^2 w (B_{y_o} y_o - B_y y)^2 \, dy}{\rho}$$

$$= \frac{2\pi^2 \ell f^2 w B_{y_o}^2 y_o^2 \left(1 - \frac{B_y y}{B_{y_o} y}\right)^2 dy}{\rho} \tag{7}$$

Finally, the loss per conductor is

$$P = \frac{2\pi^2 \ell f^2 w B_{y_o}^2 y_o^2}{\rho} \int \left(1 - \frac{B_y y}{B_{y_o} y_o}\right)^2 dy \tag{8}$$

This value is multiplied by the number of conductors in the armature to arrive at the total loss. In the present case, the total number of conductors is 72.

The integral will now be evaluated over the cross section of the conductor. By substitution,

$$\frac{B_y y}{B_{y_o} y_o} = \frac{\left(51 + \frac{1}{y^2}\right) y}{\left(51 + \frac{1}{y_o^2}\right) y_o} = k\left(51 + \frac{1}{y^2}\right) y \tag{9}$$

where k is evaluated to be 0.0624961872.

Integrating these results,

$$\int_a^b \left(1 - \frac{B_y y}{B_{y_o} y_o}\right)^2 dy = \int_a^b \left(1 - 2kB_y y + k^2 B_y^2 y^2\right) dy$$

$$= y - 2k\left[\frac{51y^2}{2} + \ell ny\right] + k^2\left[\frac{51^2 y^3}{3} + 102y - \frac{1}{y}\right] \Bigg|_a^b \tag{10}$$

$$= (b-a) - 51k\,(b^2-a^2) - 2k\,\ell\,n\,\frac{b}{a} + 867k^2\,(b^3-a^3)$$

$$+ 102k^2\,(b-a) + k^2\left(\frac{1}{a} - \frac{1}{b}\right) \qquad (11)$$

This must be evaluated for two sets of a's and b's, as shown in Figure 28. The resulting value of the integral is 2.493×10^{-10} (a computer with double-precision calculations was required for accuracy).

Substituting in the expression for the power loss,

$$B_{y_o}^{\ 2}\ y_o^{\ 2} = (3.26 \times 10^{-5})^2 \left[51 + \frac{1}{y_o^{\ 2}}\right]^2 I_f^{\ 2}\ y_o^{\ 2}$$

$$= 2.721 \times 10^{-7}\ I_f^{\ 2} \qquad (12)$$

$$\frac{2\pi^2\,\ell\,w}{\rho} = \frac{2\pi^2 \times 0.1016 \times 0.000508}{10^{-10}} = 1.019 \times 10^7 \qquad (13)$$

and

$$P = 2.772\,f^2 I_f^{\ 2} \int_a^b \left(1 - \frac{B_y y}{B_{y_o} y_o}\right)^2 dy \qquad (14)$$

$$= 6.91 \times 10^{-10}\ f^2 I_f^{\ 2} \qquad (15)$$

For 72 conductors,

$$P_{72} = 4.98 \times 10^{-8}\ f^2 I_f^{\ 2} \qquad (16)$$

The maximum value of the power loss for the active conductors occurs for the test conditions $I_f = 60$ and $f = 50$.

$$P_{72\ max} = 0.448 \text{ watt}$$

The end turn loss can be calculated in a similar way. In fact, the previous losses could have been easily calculated on a per volume basis. In the end turns, instead of the current flowing the length of the conductor and back through the superconductor, it will flow across the cross section of the conductor and back through the superconductor. In any event, the loss relationship will remain the same, provided different interpretations of the symbols are made (i.e., w is interchanged for ℓ;

ℓ is interchanged for w). The outstanding difference is in the actual values used for w and ℓ. For the end turn, ℓ should be

$$\ell = \frac{5}{6}\pi y_o = 0.226 \tag{17}$$

Therefore, the ratio of the end turn losses to the active length losses is 0.226/0.1016 = 2.22. The total losses both for the active length and for the end turns are then

$$\begin{aligned} P_{total} &= 3.22\, P_{72} \\ &= 1.604 \times 10^{-7} f^2 I_f^2 \end{aligned} \tag{18}$$

It is pertinent to point out again that this represents a worst-case analysis. In the actual case, flux redistribution would surely change this value.

Another loss results from exposing the end turns along their length to a sinusoidal, constant-amplitude moving space flux due to the field windings. The mathematical model for this loss is difficult to devise. In any event, these losses should be of the same magnitude as the other losses and as an approximation are taken equal to the other losses. The expression then for all of the losses is

$$P = 3.208 \times 10^{-7} f^2 I_f^2 \tag{19}$$

or if the appropriate expression for $B_{arm}(k_g)$ is substituted for I_f,

$$P = 1.173 \times 10^{-4} f^2 B_a^2 \tag{20}$$

Unclassified

Security Classification

DOCUMENT CONTROL DATA - R & D

(Security classification of title, body of abstract and indexing annotation must be entered when the overall report is classified)

1. ORIGINATING ACTIVITY (Corporate author) Avco Everett Research Laboratory Everett, Massachusetts	2a. REPORT SECURITY CLASSIFICATION Unclassified 2b. GROUP

3. REPORT TITLE

EXPERIMENTAL INVESTIGATION OF SUPERCONDUCTING SYNCHRONOUS MACHINES

4. DESCRIPTIVE NOTES (Type of report and inclusive dates)

Final Report

5. AUTHOR(S) (First name, middle initial, last name)

J. C. LaFrance
E. J. Lucas
J. Teno

6. REPORT DATE December 1969	7a. TOTAL NO. OF PAGES 74	7b. NO. OF REFS 15
8a. CONTRACT OR GRANT NO. DA 44-177-AMC-410(T) b. PROJECT NO. Task 1G162204A01410 c. d.	9a. ORIGINATOR'S REPORT NUMBER(S) USAAVLABS Technical Report 69-70 9b. OTHER REPORT NO(S) (Any other numbers that may be assigned this report)	

10. DISTRIBUTION STATEMENT

This document is subject to special export controls, and each transmittal to foreign governments or foreign nationals may be made only with prior approval of US Army Aviation Materiel Laboratories, Fort Eustis, Virginia 23604.

11. SUPPLEMENTARY NOTES	12. SPONSORING MILITARY ACTIVITY US Army Aviation Materiel Laboratories Fort Eustis, Virginia

13. ABSTRACT

This report details the design and testing of a synchronous motor with superconducting field and armature windings. Data are furnished on the performance of the superconducting field and armature windings. The open-circuit characteristics and terminal characteristics of the loaded machine operating as a generator with its armature in LN_2 and in the superconducting state are given. Data are given on the machine operated as a synchronous motor. The design for a number of 3000-hp motors with superconducting field winding is given.

DD FORM 1 NOV 1473 REPLACES DD FORM 1473, 1 JAN 64, WHICH IS OBSOLETE FOR ARMY USE.

Unclassified

Security Classification

Unclassified
Security Classification

14. KEY WORDS	LINK A		LINK B		LINK C	
	ROLE	WT	ROLE	WT	ROLE	WT
Superconductors Superconducting Electric Machines AC Losses in Superconductors Superconducting Motors Superconducting Generators Rotating Superconducting Fields						

Unclassified
Security Classification